

Prospects of Emerging Engineered Oxide Nanomaterials and their Applications

Jitendra Gangwar^{#,1}, Bipin Kumar Gupta[#], and Avanish Kumar Srivastava^{#,*}

[#]CSIR-National Physical Laboratory, New Delhi- 110 012, India

¹Department of Physics, The IIS University, Jaipur- 302 020, India

*E-mail: avanish.aks555@gmail.com

ABSTRACT

This review article is mainly focused the recent progress on the synthesis and characterisation of emerging artificially engineered nanostructures of oxide materials as well as their potential applications. A fundamental understanding about the state-of-the-art of the synthesis for different size, shape and morphology have been discussed in details, which can be tuned according to the desired properties of oxide nanomaterials. These tunable properties have also been discussed in details. The present review covers a wide range of artificially engineered oxide nanomaterials such as cadmium-, cupric-, nickel-, magnesium-, zinc-, titanium-, tin-, aluminium-, and vanadium-oxides and their useful applications in sensors, optical displays, nanofluids and defence.

Keywords: Nanotechnology, metal oxides, nanostructures, sol-gel, hydrothermal, co-precipitation, electron microscopy, optical, nanofluids

1. INTRODUCTION

In recent times, the existence of newly synthesised various morphologies dependent structures in the range of 100 nm are described as nanomaterials and characterised them by better properties than their micrometric analogues which have found a wide range of applications¹⁻¹⁴. Basically, nanomaterials are classified into three categories according to their source: (i) natural, (ii) incidental and (iii) engineered. Recently, engineered nanomaterials tailored with their shape, size and morphology are extensively studying in worldwide due to their outstanding properties which were limited in bulk materials. Metal oxides are the most enthralling classes of solids with a variety of structures, properties and applications in catalysts, thermal conductivity enhancers, optical devices, energy storage/conversion devices, phosphors, and extensively as sensors¹⁵⁻²⁴. Metal oxides are mainly composed of only metal and oxygen elements. The metal elements are fundamentally considered into two groups either in high melting-points *e.g.* aluminium (Al), vanadium (V), titanium (Ti) and nickel (Ni), or in low melting-points like zinc (Zn) and tin (Sn). Metal oxides demonstrate metallic, semiconducting or insulating characteristics due to their different electronic structures. In general, oxides formed by metals residing at the middle of the periodic table are semiconductors or metallic in nature (*e.g.* CuO, ZnO, NiO, TiO₂, Fe₂O₃, Cr₂O₃, *etc.*), whereas, those formed by the metals existing at the left or right of the periodic table are normally insulating in nature (*e.g.* MgO, CaO, Al₂O₃, SiO₂, *etc.*)²⁵⁻³². The nano-particles, wires, tubes, fibers, whiskers, films, layers, triangles and tetrapods of the variety of metal oxides are the most desired nanostructures for the technological applications. Metal oxide nanomaterials (MON)

with tunable coordinations of the metal cation and oxygen anion have received much attention in the scientific communities due to their unique properties relates to chemical or physical which plays a decisive role in the recent advancements of modern science and some key technologies such as nano, bio and information. These MON have four unique structural features: (i) large surface area-to-volume ratio, (ii) cations with valance states, (iii) anions with deficiencies, and (iv) depletion of carriers.

These are the fundamental bases for creating and tuning the novel material properties that have extensively applied in sensors, indicators, bio-imaging detection, optical devices, data security, missile plume detection and defence applications³³⁻⁴².

The remarkable physicochemical characteristics of these MON can be attributed to their miniaturised size (surface area, size distribution), chemical composition (crystallinity, purity), surface structure (surface-reactivity, sensitivity, and groups), porosity, shape, aggregation and defect centers (charged and neutral vacancies, F⁺ or F²⁺ and F⁰, respectively). In addition to above, reduction in crystal size would significantly increase the sensor performance and the band gap engineering by possible modification of MON which is one of the most exciting research area. Therefore, by altering these characteristics, the structural, sensing, optical and chemical properties of MON may be tuned and adapted to their potential to facilitate both fundamental research and practical applications through their advantageous chemical and physical properties⁴³⁻⁵⁰. Their novel properties can be tailored significantly by producing them at nanoscale in different morphologies.

The state-of-art of MON is an important aspect of nanotechnology. The ability to design and produce MON with new physical properties is a major challenge in nanotechnology.

Developing engineered MON with very specific properties and promising applications is a real scientific challenge through certain chemical or physical processes or both which could be used in numerous thrust areas. An entirely new concept of unique features in terms of sensing, optical-, electro-, photo-, and magnetic-properties and their applications including thermal stability and chemical resistance of MON depends on the state-of-art. Since the properties of materials strongly depend on its nanostructures that originate from their highly reduced dimensions (between the range of 1 nm - 100 nm), which is of huge interest in the field of materials science and engineering. MON are mostly functional in sensing and optical devices that gives various advantageous like high surface to volume ratio, favorable chemical stability, altered physical properties, confinement effects resulting from the nanoscale dimensions and remarkable resistivity variation in a gaseous environment. Indeed, MON has emerged as a new generation of building block materials which is beyond the conventional chemicals and expedite broad applications of the materials to modern optoelectronics and biomedical engineering, which generates the possibility of constructing nanoscale electric, optoelectronic devices and biological nanopores. Additionally, electrical conduction behaviour of semiconducting MON and excellent proton conductivity of insulating MON commonly changes at different oxygen partial pressure environments and by their dissociation of protons, making them promising component materials for a wide range of ecofriendly applications, including sensors, nanoenergy storage and conversion, optical displays, fuel cells and solar cells⁵¹⁻⁶². Moreover, various relevant existing and potential applications for MON systems make them highly attractive to researchers in worldwide.

In this review, we are elaborating on details about the structural and morphological dependence of oxide nanomaterials and their applications. Various MON that are widely used as the essential components in nanoscale devices, providing a potential platform to sensing, detecting and defense applications are investigated. The review describes systematically which covers from a brief introduction to MON and optical as well as the thermal behaviour of a few technologically relevant oxides, including CdO, CuO, NiO, MgO, ZnO, TiO₂, SnO₂, Al₂O₃, VO₂ and later explores the state-of-art of synthesis of MON through sol-gel, hydrothermal and co-precipitation approaches with their application and new challenges.

1.1 Recent Trends in Oxide Nanomaterials

Recent trends in oxide nanomaterials clearly evident a large number of MON-reliant applications emerging out in many research fields such as sensors, heat transfer science, optical devices and many more applications in the past few years. MON have shown many beneficial properties related to their chemical composition and small dimensions, etc., i.e. special sensitivity, reactivity, emission of strong tunable blue photoluminescence with high quantum efficiency and so on. The electronic structure (semiconductor or insulator behaviour) plays a seminal role in understanding, exploiting and predicting the remarkable properties of MON. In transition semiconducting MON, the oxidation state of the metal ion

generally drives the conduction towards n-type (electron) or p-type (hole). For instance, MON like CuO and NiO reveal p-type conductivity due to the oxidation state of the central metal ion, which lies in its lowest oxidation state, whereas CdO, ZnO, TiO₂, SnO₂, and VO₂ show n-type conductivity due to reduction of metal ion that have central metal ions in their highest oxidation state. Moreover, in insulating MON like MgO and Al₂O₃, associated with defects (*e.g.* point defects, intrinsic/extrinsic defects and F-centers) are produced during various synthetic methods, which may be F-luminescent centers on the surface of materials.

MON exist in different types of polymorphic (material with similar composition, but a different crystal structure) configurations. Consequently, the phases that have a higher stability in nanostructures as compared to bulk materials, establishing MON as technologically the most pronounced ceramic materials as well as in many others suitable applications such as sensing, field emission and bio-sensing potential. This crystallographic structural phenomenon has been detected in TiO₂, Al₂O₃, and VO₂ oxides. Up to now, many phases of polymorphs of MON have been reported in literature, such as eight for TiO₂ (rutile, anatase, brookite, TiO₂-B (bronze), TiO₂-R (ramsdellite), TiO₂-H (hollandite), TiO₂-II (columbite) and TiO₂-III (baddeleyite)), seven for Al₂O₃ ($\alpha \rightarrow$ alpha; $\gamma \rightarrow$ gamma, $\delta \rightarrow$ delta, $\theta \rightarrow$ theta, $\iota \rightarrow$ iota, $\kappa \rightarrow$ kappa and $\sigma \rightarrow$ sigma) and nine for VO₂ (rutile (R), monoclinic (M), triclinic (T), tetragonal (A), monoclinic (B), tetragonal (C), monoclinic (D), VO₂ with a BCC structure and paramontroseite VO₂)⁶³⁻⁸¹.

1.2 Selectivity/Suitability of Oxide Nanomaterials

MON is considered as one of the most dominant nanomaterials for nanotechnology as well as the most widely used nanomaterials in our daily life. Among the different MON; CdO, CuO, NiO, MgO, ZnO, TiO₂, SnO₂, Al₂O₃, VO₂, and many others, which are well established MON that are being used for different potential application purposes. The analysis of MON is mainly classified in two categories:

- (i) experimental characterisations
- (ii) theoretical simulations.

In experimental analysis, several structural and microstructural evolutions as well as sensing, optical and thermal properties are carried out by different crystallographic, microscopic and spectroscopic techniques. The experimental characterisation techniques provide an influential tool to determine the structure and composition of MON which is an essential requirement for understanding the properties of those materials. The state-of-the-art techniques used in structural, morphological, thermal and optical evaluations include X-ray diffraction, scanning electron microscopy, high-resolution transmission electron microscopy, helium ion microscopy, thermal conductivity, UV-Visible and photoluminescence spectroscopy. The characterisation of such nanostructures is discussed in this section, accompanied by the crystal structure and display of images of MON by scanning electron microscopy (SEM) and high-resolution transmission electron microscopy (HR-TEM).

Some most popular and highly useful MON are discussed and described as follows:

1.2.1 Cadmium Oxide (CdO) Nanostructures

CdO has a cubic crystal structure [space group $Fm\bar{3}m$] with a unit-cell length of 0.469 nm. It has a face-centred cubic structure (NaCl type) with alternating cadmium (Cd) and oxygen (O) atoms located at lattice points. CdO is a unique wide band gap n-type semiconductor ($E_g = 2.4$ eV) possessing excellent electrical, mechanical and optical properties. CdO is a promising candidate for gas sensors, optoelectronics, solar cells, phototransistors, photodiodes and transparent electrodes.

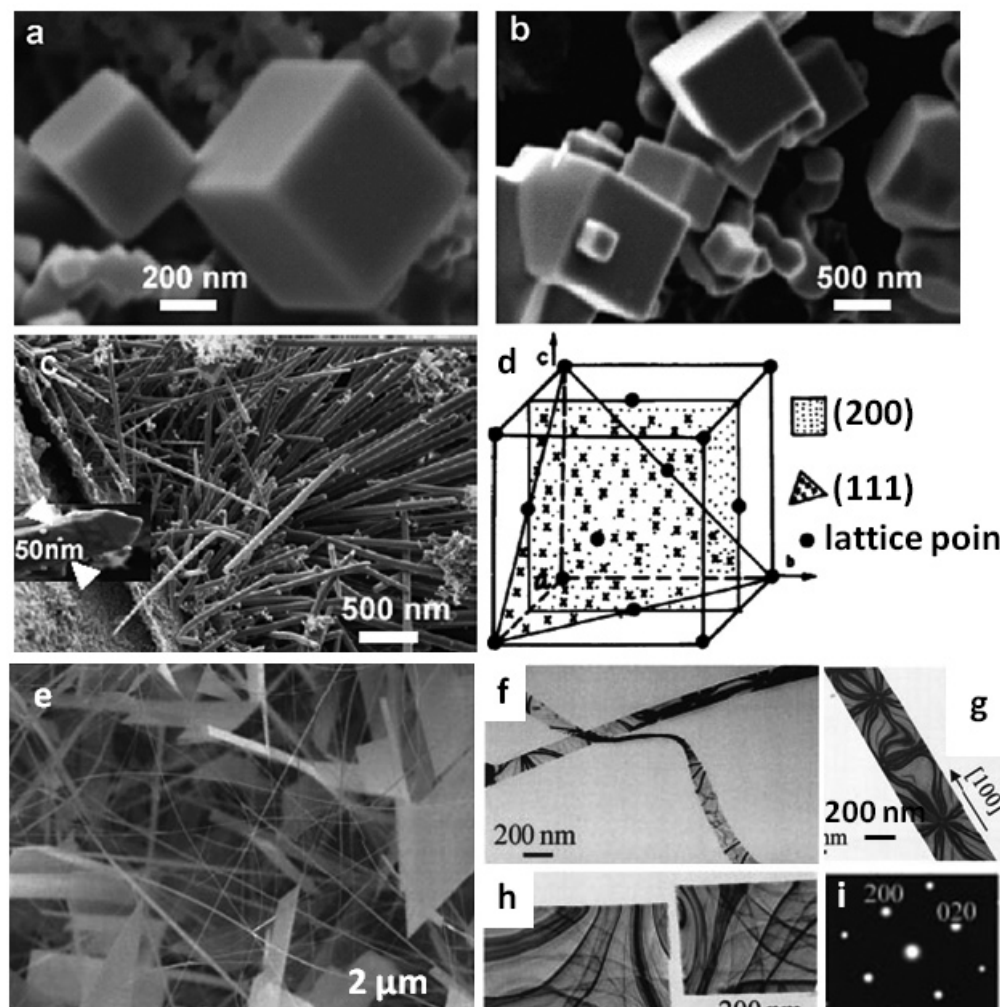


Figure 1. SEM micrographs showing different size cuboids (a, b), nanorods (c), nanobelts and sheets (e). (f and g) display the TEM images of CdO nanobelts growing along [100]. (h) A broken CdO nanobelt as a result of focused electron beam illumination. (i) Electron diffraction pattern of the single crystalline CdO. (d) Schematic of unit cell of CdO crystal marked with (200), (111) planes and lattice points. Inset (c) shows a corresponding a nanotip of CdO^{19, 57}.

1.2.2 Cupric Oxide (CuO) Nanostructures

Copper (II) oxide (cupric oxide; CuO; known as tenorite in its mineral form) inherently has a potentially huge application as an electrode material in Li-ion batteries as well as outstanding structural and physicochemical properties for practical applications such as in hazardous gas sensing, as a crucial component in high temperature superconductors and thermal conductivity improvers in nanofluids. CuO has a monoclinic

crystal structure [space group $C2/c$] with lattice parameters of 0.468 nm, 0.342 nm, and 0.513 nm, $\beta = 99.549^\circ$. Unlike the other 3d transition metal monoxides, which have a cubic rock salt crystal structure with an octahedral coordination, CuO is a unique monoxide and has a square planar coordination of the Cu atom to the neighbouring oxygen atoms. It is a narrow band gap, varying between 1.2 eV - 1.8 eV, p-type semiconductor material which can prove attractive deviation from its bulk counterparts when obtained in a nanoscale dimension.

1.2.3 Nickel Oxide (NiO) Nanostructures

Amongst different transition metal oxides, which can be used in electrochemical capacitors, nickel oxide (NiO; referred to as bunsenite in its mineralogical form and classified as a basic metal oxide) is highly suitable for energy conversion as well as storage devices and favoured as anode materials because of its high theoretical specific capacitance of 2584 F g⁻¹, low cost with highly biocompatible. NiO in bulk crystals has a rhombohedral crystal structure and antiferromagnetism (in which the electronic wave-functions of magnetic Ni²⁺ ions overlap with those of the intermediate nonmagnetic O²⁻ ions) below Néel temperature (T_N of 250 °C), while the nanometer-sized NiO structures possess cubic crystal symmetry and exhibit paramagnetic behaviour above that temperature. As a 3d transition metal oxide p-type semiconductor with a wide band gap of 3.6 eV - 4.2 eV, NiO adopts cubic structure [space group $Fm\bar{3}m$] with a unit-cell length of 0.417 nm in octahedral environment of the Ni²⁺ ($3s^23p^63d^8$) imposed by the six neighbouring oxygen (O²⁻) ions. The non-stoichiometry (Ni_{1-x}O or NiO_{1-x}) in NiO is followed by a colour change and electronic structure. Curiously, the non-stoichiometric NiO exists

in black/greyish texture with semiconducting nature whereas the stoichiometrically NiO being green color and insulating behaviour. However, due to available nonstoichiometry in NiO determines the achievable specific capacitance ranged from 50 F g⁻¹ to 411 F g⁻¹. NiO, an alternative of RuO₂, with various morphology including nano-particles, flowers, slices, petals, belts, wires, capsules and many others have received a lot of interest regarding their superior functionality and nonvolatile memory characteristics including gas sensing, optical,

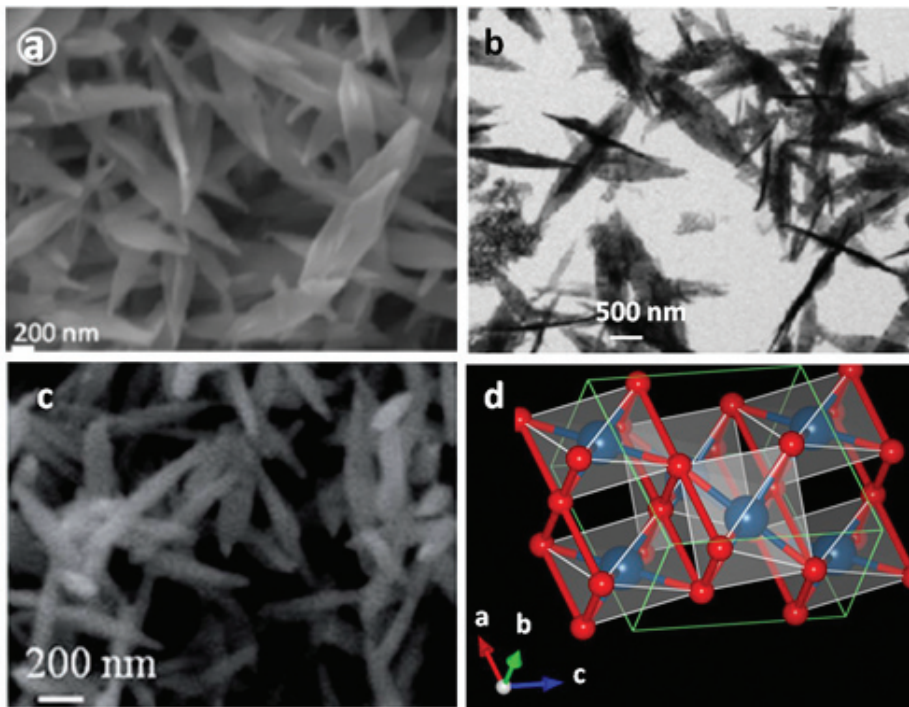


Figure 2. (a) SEM and (b) HRTEM micrographs of CuO nanoparticles, (c) SEM image of the ellipsoidal shaped CuO nanoparticles. (d) CuO monoclinic unit cell; colour code: the blue balls indicate Cu atoms and the red balls indicate oxygen atoms^{50, 77}.

1.2.4 Magnesium oxide (MgO)

Nanostructures

Speaking of MON, particularly those of alkaline earth metals, such as CaO, BeO, MgO, and SrO, are highly sought in material science after for their widest and most fascinating range of properties among any single class materials. Magnesium oxide (MgO) is among the simplest oxides constituting the rocky mantles of terrestrial planets such as Earth and the cores of Jupiter and other giant planets. MgO is one of the most abundant phases in planetary mantles, and is regarded amongst the most promising alkaline earth-based oxides that is attracting attention due to its high economical availability, toxicity and ecofriendly nature, and has been utilised as an inorganic phosphor for optoelectronics devices, biosensors for liver cancer immunoassay, catalyst for methane oxidation and solid-state lighting applications due to their defect-induced luminescence properties. In addition to this, MgO is one of the most important metal oxides and, as a typical wide electronic band-gap insulator ($E_g =$

electrochemical, field emission and magnetic properties. As a consequence of their high thermal/chemical stability, superior reversibility and stability in alkaline solution, high pseudocapacitive behaviour, p-type and wide-range engaging properties, NiO nanostructures are excellent for utilise in batteries, gas sensors, humidity sensors, supercapacitors, memory devices, high energy density devices, antibacterial materials, electrochromic materials, *etc.*

7.8 eV) and smooth surface features, which allow it to act as persistent application in sensors, catalysis, refractory, paint, toxic waste remediation and superconductors. MgO possesses a cubic crystal structure [space group $Fm\bar{3}m$] with lattice parameters of 0.419 nm in hexa-coordinated Mg^{2+} cations and O^{2-} anions. Moreover, the F-center defect in MgO (also called the anion vacancy) is a typical example of a classical intrinsic point defect in binary ionic compound insulators, which is

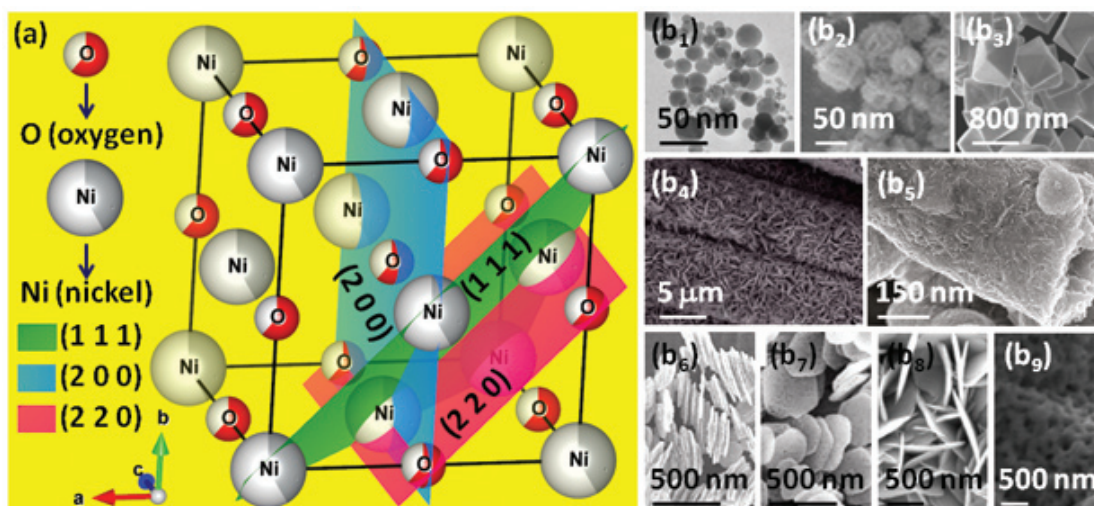


Figure 3. (a) Crystallographic representation of cubic NiO; the grey and red balls represent nickel (Ni) and oxygen (O) atoms, respectively. The green, blue and pink rectangles indicate (111), (200) and (220) lattice planes, respectively. (b₁-b₉) demonstrate several NiO nanostructures: NiO nano-particles (b₁), -flowers rose-like (b₂), -crystals with octahedral morphology (b₃), -flakes (b₄), -tube (b₅), -columns (b₆), -plates (b₇), -walls (b₈) and -porous morphology (b₉)^{11,16,22,46,56,72,76,83}.

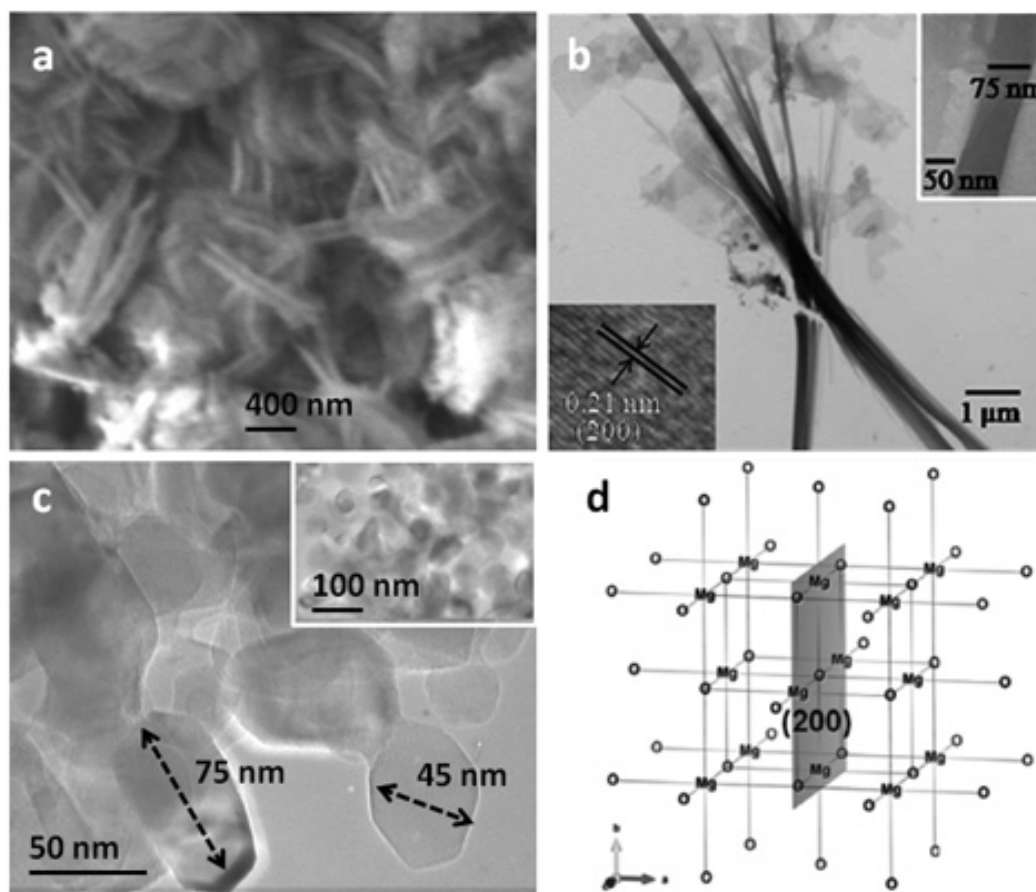


Figure 4. High-magnification SEM image of the MgO nanofibers (a), bright-field TEM image of MgO-nanofibers (b) and nanoparticles (c). Insets: (b) illustrate the corresponding high-magnification view (in the right upper inset) and well-defined lattice fringes with a d-spacing of 0.21 nm corresponding to the [200] plane (in the left lower inset), and (c) corresponding lower magnification image. Illustration (d) of the (200) facet of cubic-MgO (note the alternating layers of Mg²⁺ and O²⁻ ions); atoms for magnesium and oxygen are represented by Mg and O, respectively⁵⁹⁻⁶⁰.

directly or indirectly responsible for many of the material's properties. MgO is commonly used material with applications in a diverse range of areas from electronics to microelectronics to optoelectronics to photovoltaics.

1.2.5 Zinc oxide (ZnO) Nanostructures

Semiconducting MON with one dimensional (1-D) morphology (*e.g.* nanowires, nanorods and nanotubes) are indispensable components for the realisation of nanoelectronics and exhibit highly tunable coordination of cation and anion as well as optical properties that make them attractive for broad applications; especially in a variety of sensors. Among these, zinc oxide (ZnO) is an important nanostructure, as it could be the next most important nanomaterial after the carbon nanotubes, for short wavelength optoelectronics and a variety of sensors. Oxide nanostructure of ZnO is one of the most promising nanomaterials in integration of nanosystems and biotechnology. It is a direct wide band gap (~ 3.3 eV - 3.6 eV) n-type semiconductor with large electron mass $\sim 0.3 m_e$ (m_e : bare electron mass), thermal energy at room temperature (26 meV) and strong exciton binding energy (60 meV), which is expected to exhibit an efficient exciton emission at room temperature under low excitation energy. This produces ZnO useful in a number of photonic applications. Besides, ZnO is an

important low cost, ecofriendly basic semiconductor material, which is used considerably in nanoscale device fabrication of sensors, optics and optoelectronics for its excellent sensing, optoelectronic, chemical and thermal stability, and photo-electrochemical properties. ZnO has a wurtzite hexagonal crystal structure [space group $P63mc$] with lattice parameters of 0.325 nm and 0.520 nm having a number of alternating planes of fourfold coordinated O²⁻ and Zn²⁺ ions, stacked alternatively along the c-axis, with high density (5606 kg m⁻³). ZnO-based-1D nanostructures (ZnO-nanowires, nanoneedles, nanoflowers, brushes, dendrites and tetrapods morphology) have gained substantial research interest owing to its abundance and some of their particular advantages such as high contrast ratio, high ambient visibility, high image resolution, good heat resistance and low out gassing, realise better photonic and electronic devices for sensing applications.

1.2.6 Titanium Dioxide (TiO₂) Nanostructures

Since the discovery of photocatalytic properties of titanium dioxide (TiO₂; commonly referred to as titania) by Honda-Fujishima in 1967, TiO₂ is almost the only material suitable for industrial use at present and also probably in the future. Among the various polymorphic modifications, the highly crystalline rutile, anatase and brookite-TiO₂ are the most popular and widely

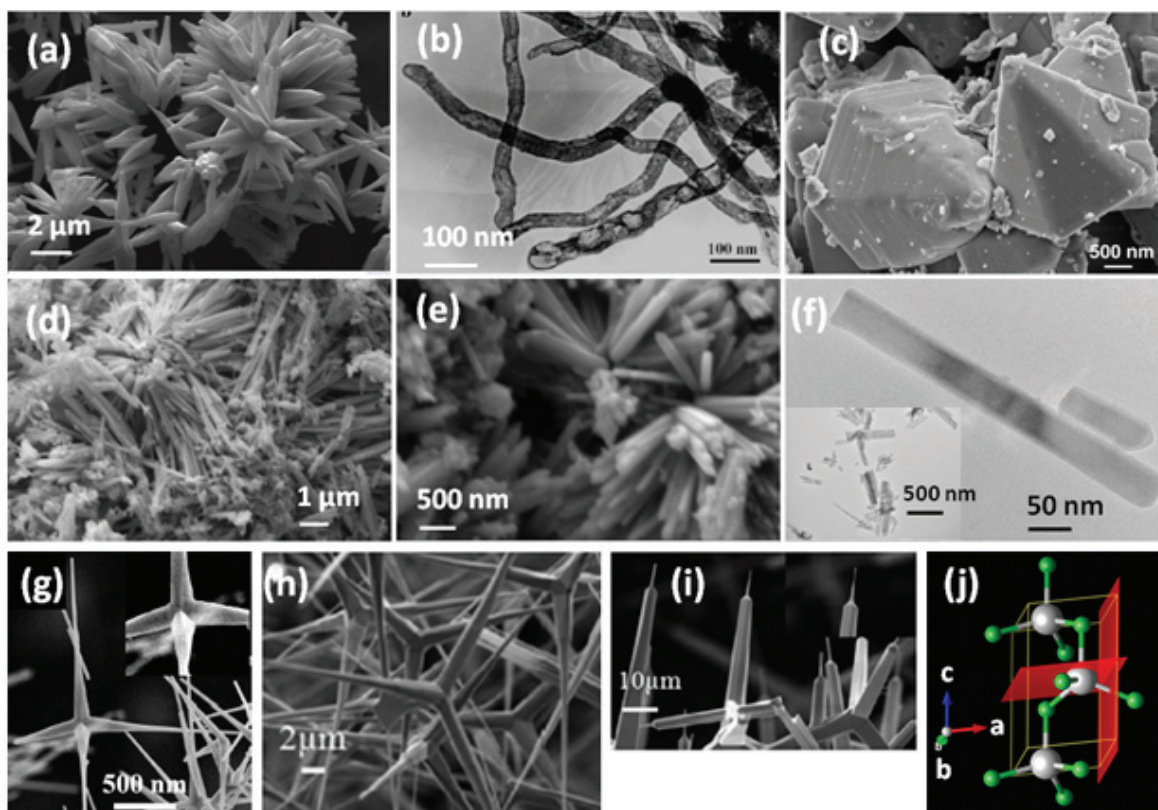


Figure 5. SEM image of ZnO nanoneedles (a), TEM micrograph of porous ZnO nanowires (b), SEM images of ZnO displaying faceted pyramid-shaped growth (c), nanorods (d and e), bright-field TEM image of ZnO nanorods (f), SEM images of ZnO-tetrapods (g, h and i). The crystallographic ball-and-stick model of ZnO (j); color code: green (small) balls indicate oxygen atoms and white (large) balls signify zinc atoms, and red rectangle represents (001) plane. TEM micrographs of ZnO nanowires (h) and nanobelts (i) showing their geometrical shape. Insets: (f) demonstrates the TEM image at low magnification of ZnO nanorods and (g) shows a central-growth region of a ZnO-tetrapod^{33,58,63-64,67-68}.

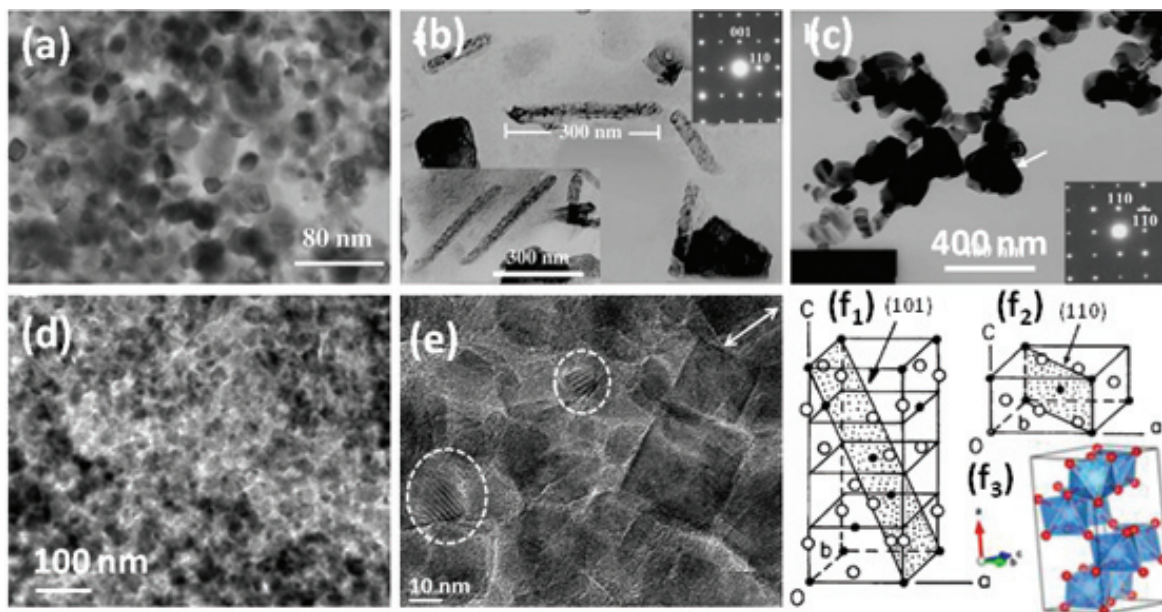


Figure 6. TEM bright field micrographs of TiO₂-nanoparticles (a), nanowires and fibrous grains (b), dendritic growth (c), uniform distribution (d) and a high magnification image (e) showing cuboid shape or thin sheets. (f) Crystallographic representation of (f₁) anatase-, (f₂) rutile-, and (f₃) brookite unit cells marked with [101] and [110] planes and lattice points. Red (small) and white (large) spheres are O and Ti atoms, respectively. Insets are SADPs from (b) rutile along [110] and (c) anatase along [001] zone axes^{54,61,68}.

used. Among these phases, rutile is the most compact and stable structure. Each unit cell contains three dimensionally arranged TiO_6 octahedra. These phases are typically used as an efficient photocatalyst for the degradation of contaminants in solution, purification of water, *etc.* Anatase TiO_2 adopts a body-centered tetragonal crystal structure [space group $I41/amd$] with lattice parameters of 0.377 nm and 0.948 nm. The brookite- TiO_2 is orthorhombic [space group $Pbca$] with lattice parameters of 0.919 nm, 0.546 nm, and 0.515 nm, whereas the rutile- TiO_2 has an orthorhombic crystal structure [space group $P42/mnm$] with lattice parameters of 0.458 nm and 0.295 nm. The three polymorphs of TiO_2 differ in how they share the adjacent TiO_6 octahedral coordination. In anatase and brookite- TiO_2 , the TiO_6 units are connected through the edges of the neighbouring units, while vicinal octahedral units share one corner in [100] direction for rutile- TiO_2 , and consequently the band gaps (3.15 eV for anatase and 3.0 eV for rutile- TiO_2) differ slightly. The applications of TiO_2 pertaining to engineering, semiconducting and medicinal industries are enormous and expected to enhance by manifold times if material is nanostructured to design fundamental nanodevices. Owing to its exceptional properties, such as visible light photocatalytic activities, high chemical inertness, higher stability, lower cost, biocompatibility, non-toxicity and environmentally friendly character, the utility of n-type TiO_2 nanostructures have been explored as a versatile material, required for sensors, thin film optical devices, biocompatible surgical instruments, photoelectrochemical, photocatalysis for the remediation of organic pollutants, pigments and dyes. Apart from this, it has been shown that the diverse properties and several applications of TiO_2 may be influenced by crystal structure, surface area, band gap and porosity.

1.2.7 Tin dioxide (SnO_2) Nanostructures

Tin dioxide (SnO_2) is an important functional material and drawn considerable attention in the scientific community for their practical use in industries as a technological component. Owing to its many remarkable physicochemical properties including excellent receptivity variation in gases, electrical conductivity, optical transparency and chemical stability as well as low efficiency in excitation and recombination process and allows minimum energy transition from valence to conduction band, SnO_2 has been suitable for large number of application in gas sensors, ethanol sensors, optoelectronic devices, transparent electrodes and heat mirrors. SnO_2 adopts a tetragonal rutile structure [space group $P42/mnm$] with lattice parameters of 0.474 and 0.318 nm. Amongst direct band gap materials, SnO_2 is one of the efficient n-type semiconductor materials and possess a wide band gap of 3.57-3.93 eV. The engineered gas sensors based on nanosized SnO_2 leads to advantages of low operating temperature and high sensitivity, offering the desirable characteristics of cheapness, simplicity and process reproducibility for gas sensing technology. Gas sensors based on 1D SnO_2 nanostructures (*e.g.* SnO_2 -nanobelts, nanowires, nanoribbons and nanowhiskers) have been growing exponentially every year, possibly owing to the convenience of obtaining large quantities of SnO_2 .

1.2.8 Aluminium Oxide (Al_2O_3) Nanostructures

Aluminium oxide or alumina (Al_2O_3), the most used oxide ceramic material and owing to its special properties, such as contains both amorphous and crystalline phases, large electronic band gap (~ 8.8 eV), high sensitivity and fast response/recovery time to humidity, excellent dielectric properties, high thermal,

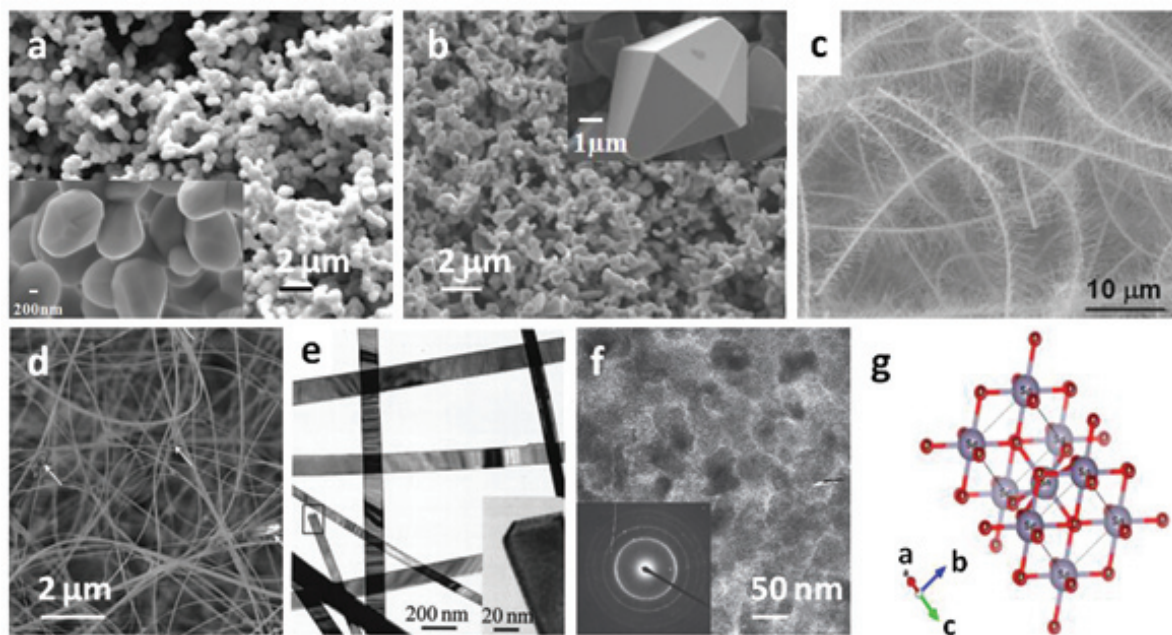


Figure 7. SEM micrographs of SnO_2 -nanoparticles (a, b) showing fine topographical feature, brushes (b). TEM images of SnO_2 nanobelts (d-e) with straight and twisted shapes, an enlargement of a broken nanobelt is inserted in (e) to display the rectangle-like cross section, SnO_2 thin film (f). Crystal structure representation of SnO_2 (h), tin (Sn) atoms are depicted in purple (large spheres) and oxygen (O) atoms are in a red (small spheres) color. Insets: (a) corresponding SEM topographical feature at high magnification, (b) a single octahedral structure of SnO_2 and (f) corresponding electron diffraction pattern of the film^{19,35,42,78}.

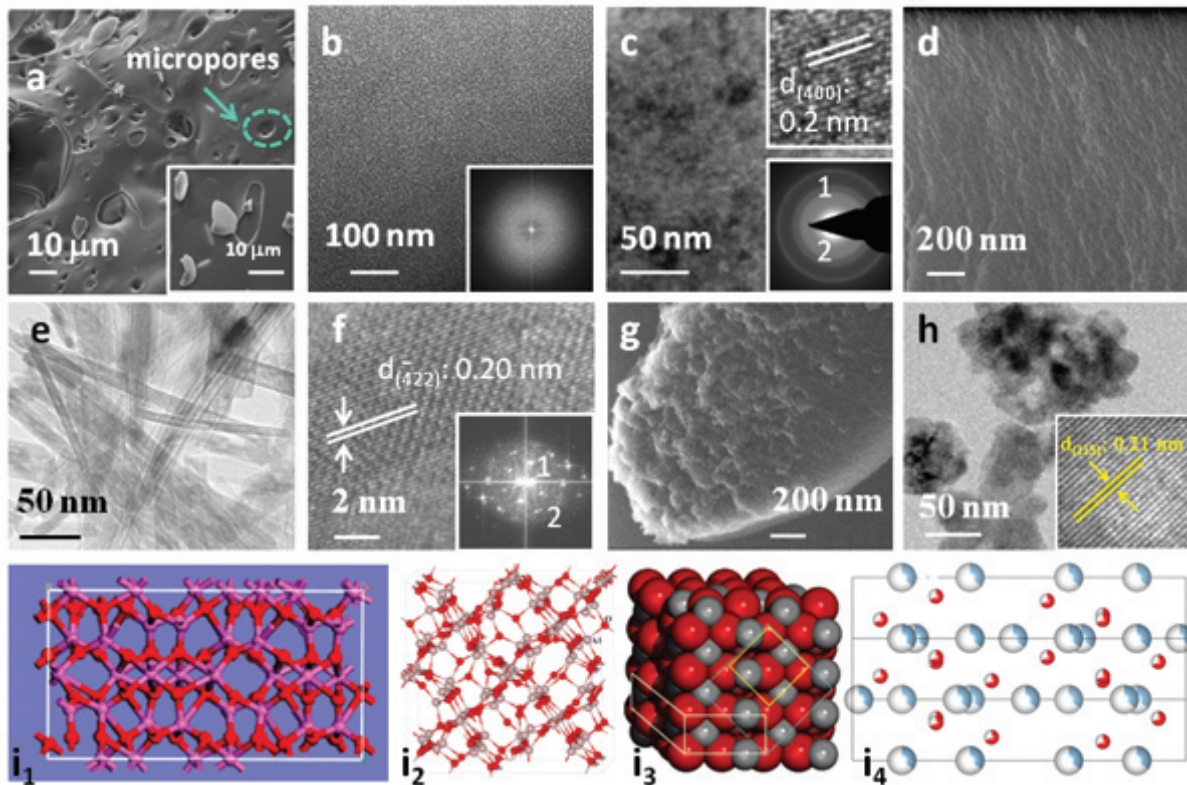


Figure 8. (a) SEM and (b) HR-TEM micrographs and the corresponding SAED pattern of amorphous- Al_2O_3 nanoparticles, (c) HR-TEM and (d) HeIM images of γ - Al_2O_3 nanoparticles, (e) bright-field TEM image and (f) lattice scale fringes of θ - Al_2O_3 nanowires, (g) HeIM image and (h) TEM micrograph of α - Al_2O_3 nanoparticles. Insets represent; (c) lattice scale fringes (the upper-right inset in c) and SAED pattern (the bottom-right inset in c) of γ - Al_2O_3 nanoparticles, (f) FFT pattern of θ - Al_2O_3 nanowires and (h) lattice scale fringes of α - Al_2O_3 nanoparticles. (i_1 - i_4) represent the atomic structure of (i_1) amorphous-, (i_2) γ -, (i_3) θ - and (i_4) α - Al_2O_3 ; color code: red spheres (i_1 - i_4) show oxygen and purple (in i_1), pink (in i_2), grey (in i_3) and blue-white (in i_4) spheres represent aluminium atoms. In i_3 , the yellow solid line shows the face-centered-cubic structure of oxygen, the white solid line marks the monoclinic unit cell of θ - Al_2O_3 , and the dotted line shows the scheme of the spinel unit cell^{4,21,49,73,79}.

mechanical and chemical stability; make it as a material of outstanding performance. The crystalline- Al_2O_3 has several metastable structural phases such as γ -, η - Al_2O_3 (cubic spinel structure), δ - Al_2O_3 (tetragonal structure), θ - Al_2O_3 (monoclinic structure), κ - Al_2O_3 (orthorhombic structure), χ - Al_2O_3 (cubic or hexagonal structure), β - Al_2O_3 (hexagonal structure) and α - Al_2O_3 (corundum); a stable phase with a rhombohedral structure. Amorphous- Al_2O_3 usually composed of random distribution of aluminium (Al^{3+}) ions and vacancies over tetrahedral (AlO_4), polyhedral (AlO_5), and octahedral (AlO_6) sites. Amorphous Al_2O_3 nanomaterials reveal bright bluish-white emission, high sensitivity and fast response/recovery time to humidity and higher thermal conductivity than their ethylene glycol based-fluid and have found extensive application in modern society for information displays and lighting, various complicated environments for fast detection of humidity, efficient energy transfer in nanofluids and suitable for fluorescent biological probes. The mixture of AlO_6 (62.5 %) and AlO_4 (37.5 %) with corner sharing oxygen atoms determines the γ - Al_2O_3 crystal phase. For the θ - Al_2O_3 phase, Al^{3+} ions is evenly distributed between AlO_4 (50.0 %) and AlO_6 (50.0 %) sites in the oxygen lattice. The iota-alumina (ι - Al_2O_3) possesses an orthorhombic lattice and the structure adjusts to include AlO_5 and AlO_3 units. For ι - Al_2O_3 , there are 22.9 % AlO_6 , 10.4 % AlO_5 , 60.4 % AlO_4

and 6.25 % AlO_3 . It is only the Al^{3+} ions in AlO_6 units that establish the thermodynamically stable α - Al_2O_3 crystal phase. Moreover, the F^+ centers (oxygen vacancies with one electron) are the most probably responsible for the ultraviolet and blue photoluminescence emission from the α - Al_2O_3 nanostructures. As a consequence, the sensing, optical, thermal and other performances of Al_2O_3 nanomaterials depend not only on their crystal phase, but also on the definite crystal facet depicted by their shape.

1.2.9 Vanadium Dioxide (VO_2) Nanostructures

Many oxides of vanadium, including VO_2 , V_2O_3 , V_2O_5 , and V_6O_{13} , possess many interesting characteristics that have created extreme interest amongst the scientific and engineering fraternity mainly due to their different polymorphs and metal to insulator transitions. Within the vanadium oxides family, vanadium dioxide (VO_2) has been able to carve a special interest mainly due to its structural phase transitions, field emission and bio-sensing potential. Additionally, one of the most compelling metal oxides is VO_2 , which undergoes a Mott metal-insulator transition (MIT) near $T_{\text{MIT}} = 67^\circ\text{C}$. Below T_{MIT} , VO_2 (I) has a low-temperature insulating monoclinic phase [space group $P21/C$] with band gap of 0.7 eV, whereas above T_{MIT} , VO_2 (M) transforms to a high-temperature metallic tetragonal phase

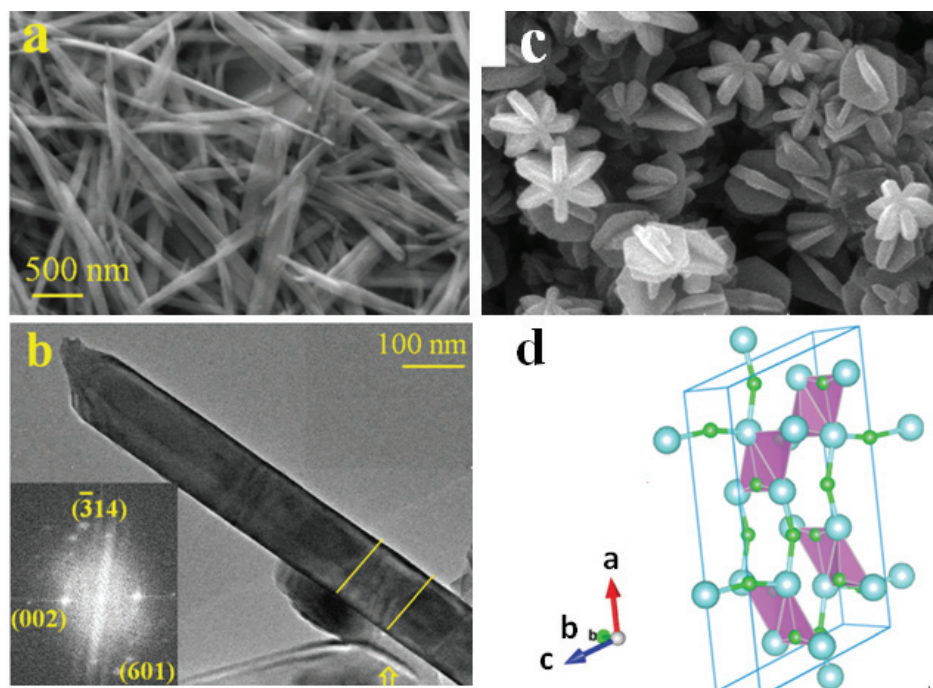


Figure 9. (a) SEM image portraying the jute-stick-like morphology of VO₂ (B) nanoparticles, (b) TEM image depicting the VO₂ (B) nanorods, (c) SEM image of VO₂ depicting the hexangular starfruit-like morphology. (d) Polyhedral structure of monoclinic VO₂ (B), the Blue balls represent vanadium (V) atoms and the green balls represent the oxygen (O) atoms.^{41, 51}.

[space group $P42/mnm$], accompanied by dramatic changes in its electrical and optical properties. VO₂ (B) has monoclinic crystal structure [space group $C2/m$] with lattice parameters of 1.206 nm, 0.369 nm, and 0.642 nm, $\beta = 106.98^\circ$ having a layered structure in which distorted VO₆ octahedra share both corners and edges. Intriguing characteristics and phase behaviour aside, VO₂ (B) has been an attractive material for nanotechnology that are widely expected to have great potential to be used in the sensors, next generation rechargeable batteries, electronic applications such as ultrafast switches, field effect transistors and also as a thermochromic material. VO₂ nanowires might be used as building blocks for functional nanoscale devices such as temperature sensors and nanoscale Mott field effect transistors. Various nanotextured VO₂ (B) materials, including nanowires, nanobelts, nanorods, nanoneedles and nanoribbons represent a particularly attractive material for humidity and gas sensors as well as dramatic change effect on the thermal conductivity of nanofluids.

A summary of various MON with their properties and applications is as shown in Table 1.

2. DIFFERENT METHODOLOGY FOR SYNTHESIS OF MON

Keeping in view of their gamut of applications, especially for efficient MON-based sensors and optical devices, it is of importance to fabricate MON of desired shapes and even multidimensional structures with large surfaces compared to the volume of the material. Properties of solid materials with size in the microscopic scale are well studied and characterised. But when their sizes shrink to dimensions of approximately 1 nm - 100 nm, the size and shape of metal oxides profoundly affect their reaction performance. Such structures are called

nanoparticles, nanowires, or nanoclusters, depending on their shape and dimensionality. Unique surface properties of MON of definite shape and size have motivated the researchers to explore new synthesis strategies for the nanostructured materials under controlled synthesis conditions. Thus, the technological challenge moved to the fabrication of metal oxides particles on the nanometre scale, which maintained their stability over long-term operation at high temperature. In order to improve versatility in advanced applications, MON-based devices for different purposes are highly desirable. MON synthesis has occupied a major part of materials science research for the last couple of decades. Various synthetic strategies have been used to synthesise MON, and many have the potential to meet the specific requirements for sensors and devices in terms of both activity and selectivity. The synthetic approaches can also be classified according to the branches of science involved physical and chemical. There are two fundamental strategies for engineering the MON;

- (i) Bottom-up approach, where MON are made up by atom by atom or molecule by molecule or more at the will of their creators,
- (ii) Top-down approach, which is more traditional MON making process, where MON are synthesised by tearing down bulk materials gradually until they get reduced to nano-sized objects.

The bottom-up approach has two major branches, physical and chemical, based on which field of science plays the dominant role in the overall outcome of the synthetic method. The top-down approach is essentially a miniaturisation technique, one that is unquestionably the most important approach from an economic point of view. Consequently, proper MON systems with desired morphology are quite

Table 1. Summary of Various Oxide Nanomaterials with their properties and applications

Metal oxides	Properties	Advanced Applications
Cadmium oxide (CdO)	High density (8150 kgm ⁻³), melting point (1500 °C), excellent electrical, mechanical and optical properties	gas sensors, optoelectronics, solar cells, phototransistors, photodiodes and transparent electrodes
Cupric oxide (CuO)	Photoconductivity, field emission and photovoltaic properties	Electronics, sensors, magnetic storage media, optical, batteries,
Nickel oxide (NiO)	High chemical and thermal stability, environmental benignity, gas sensing, electrochemical, optical and field emission properties	In supercapacitors, catalysis, lithium-ion batteries, thermal conductivity enhancement of ethylene glycol based nanofluids
Magnesium oxide (MgO)	High surface area, facile mass transport, recycling, eco friendliness and low cost	In metal oxide semiconductor gate controlled devices, paints, nanooptics, advanced ceramics and optical devices, as a refractory material, unreactive substrates, indicators and photon sources, for water purification
Zinc oxide (ZnO)	Detection of UV and IR radiation, UV protection, wide band gap with large exciton binding energy (60 meV), high: contrast ratio, ambient visibility, image resolution, a good heat resistance, reduce photoaging, low out gassing	In light emitting diode (LED), photo detectors, night vision systems, flame temperature sensing, missile plume detection, space to space communication, luminescence devices, the next generation of uv lasers, electronics, sensors, drug delivery, biomedical imaging, optoelectronic devices, chemical sensors
Titanium dioxide (TiO ₂)	Electrochemical and photoinduced properties, high: photocatalytic activity, chemical stability, non-toxic, being commercially available	Photocatalysis, electrochemical energy Storage, in white pigments, as support in catalysis, cosmetics or toothpastes, as electrode material lithium ion batteries
Tin oxide (SnO ₂)	High receptivity variation in gases, low electrical resistivity, high optical transparency and excellent chemical stability, large exciton binding energy (130 eV)	Gas sensors, catalyst for biosensors, catalyst carrier for fuel cells, anode material in li-ion batteries, solar cell, light emitting diodes, as a transparent conductor in gas sensor, transparent electrodes for solar cells, heat mirrors, optoelectronic devices, catalysts.
Aluminium oxide (Al ₂ O ₃)	Exists in several polymorphs, excellent porosity, high specific surface area, surface acid-base characteristics, negative surface energy, superior wear resistance, mechanical strength, hardness, and refractoriness, low electric conductivity	Catalyst supports in refining, used as soft abrasive, adsorbents, widely employed in miniature power supply, ceramics, petro-, fine-chemicals, structural composites for spacecraft, automotive and petroleum industry, fast optical sensing/switching devices, highly suitable for ferroelectric liquid crystal based display applications, catalyst supports for high temperature reactions, cutting tools, polymer composites, coatings, varnishes, advanced ceramics and paints.
Vanadium oxide (VO ₂)	Low cost, relatively low toxicity, electrochemical, electrical transport, field emission and bio-sensing properties	In lithium-ion batteries as cathode materials, electric vehicles (EVS) or hybrid EVS, electronic applications, ultrafast switches, field effect transistors, solid state memory and also as a thermochromic material.

difficult to obtain via bottom-up strategy method because it requires sophisticated instruments and complicated reaction process. MON can be synthesised by bottom-up approaches have been most widely adopted mainly due to its advantages such as simplicity, inexpensive instrumental setup, easy operation, low-reaction time, high yield production and good control over the experimental conditions, which are favorable from the viewpoint of practical application. These features often lead to differences in physical properties and performance of MON. On the other hand, synthesis of 1-D MON such as nanowires, nanorods, nanotubes, nanobelts, nanofibers and fibrous grains requires development of novel methods with potential applications in numerous areas such as gas sensing, optoelectronics and nanoscale devices. The smaller-sized nanocrystallites offer short-range interfacing between solid-particle and liquid phase and are beneficial for higher thermal conductivity enhancement in nanofluids. High surface area materials provide a large interface for any type of reaction, *e.g.* physisorption of water vapors and ensure higher adsorption of water molecules leading to a greater density of charge carriers. Therefore, it is essential to develop synthetic approaches that allow for a systematic selection of the crystalline phase, particle

size distribution, porosity, morphogenesis, defect centers and degree of aggregation. The synthesis processes to amorphous and typical crystalline polymorphs structures of MON include amongst others the sol-gel or even hydrothermal approaches, template free wet chemical solution and precipitation methods become increasingly popular in recent years due to several advantages, such as smaller particles sizes and that high purity materials can be obtained. Table 2 provides an overview of the selected synthesis routes and various MON that are typically accessible through these approaches.

2.1 Sol-Gel Processing

Amongst top-down approaches thorough solution-based chemical synthesis routes, sol-gel technique of MON is of particular interest due to its inexpensive, low-reaction time and reliable way that can be reproducible with consistent size distribution. The sol-gel technique is a simple as well as universal synthesis method and entails the development of MON through colloidal solution (sol) and the gelatinised colloidal solution (gel) in liquid phases. The colloidal solution (sol) acts as the precursor for the MON (gel). Explicitly, when the liquid is removed from sol, the sol becomes a gel. This method starts with

Table 2. Summary of Various Synthesis routes of MON

Metal oxide	Nanostructure	Synthesis routes
CdO	Nanorods, nanotip, cuboids	Solid-vapour deposition technique ^{19,57}
CuO	Nanoparticles, nanoellipsoids	Wet chemical solution method ^{50,77}
NiO	Nanoparticles, porous	Hydrothermal, wet chemical solution ⁴⁶
MgO	Nanoparticles, nanoflakes/nanofibers	Co-precipitation/ wet chemical solution method ⁵⁹⁻⁶⁰
ZnO	Nanorods, tetrapods, thin film	Sol-gel, solid-vapour deposition ^{33,58,63,67-68}
TiO ₂	Nanoparticles, cuboid shape	Sol-gel, solvothermal ^{54,61,68}
SnO ₂	Nanoparticles	Sol-gel, hydrothermal ^{19,78}
Al ₂ O ₃	Nanoparticles, nanowires	Sol-gel, hydrothermal ^{4,18,73}
VO ₂	Nanorods	Hydrothermal ^{41,51}

the precursors that are chosen to make a gel having a uniform distribution of cations. The reactive precursors, typically metal alkoxides or metal salts (such as nitrates and chlorides), usually surrounded by various reactive ligands. The sol-gel synthetic route based on the various processes of controlled hydrolysis and condensation reactions of appropriate metal precursors. Here the starting material in the sol is hydrolysed to produce the corresponding hydroxide in contact with liquid water or alcoholic solution. Condensation of hydroxide molecules with removal of the liquid water or alcoholic solution from the sol yields a gel, and the sol/gel transitions control the particle size and shape. Further heat treatment (calcinations or annealing or drying) of gel (hydroxide) produces the corresponding nanostructures of metal oxides. Some typical examples are as follows: CdO nanorods, MgO nanoparticles, ZnO-nanorods, thin films and tetrapods, TiO₂ nanoparticles with cuboid shape, Al₂O₃ nanoparticles and VO₂ nanorods.

2.2 Hydrothermal Synthesis

As MON find a huge amount of applications in mediating the interaction between sensing and optical devices, hydrothermal synthesis has emerged as a scalable alternative to vapour-phase techniques for producing 1-D MON with excellent crystal quality and morphogenesis. The hydrothermal technique has long caught the imagination of researchers to directly prepare nanometre-sized crystalline powders because it provides a very good compositional and morphological control over the product properties. Hydrothermal synthesis refers to the various techniques of crystallising substances from high-temperature aqueous solutions where the solvent is heated above the normal boiling point in a sealed reaction vessel. It is very similar to the solvothermal synthesis, the difference between the two synthesis processes being in the precursor solutions. The method is called solvothermal synthesis when any solvent other than water is being used. In a

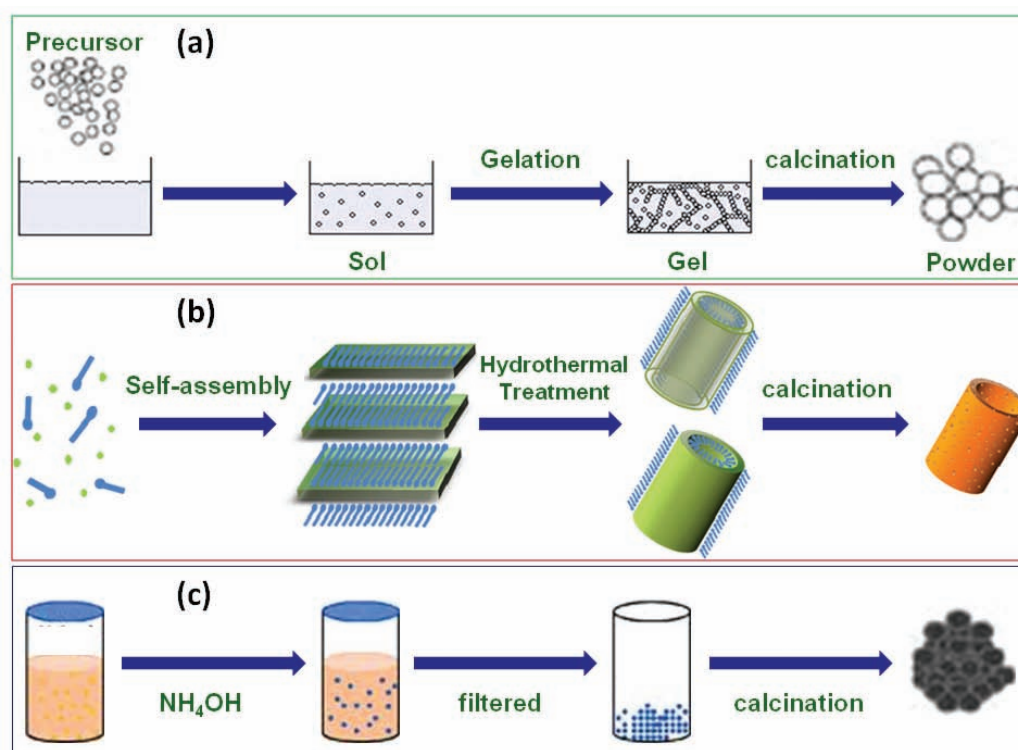


Figure 10. A schematic representation of the chemical synthesis of MON via (a) sol-gel, (b) hydrothermal, and (c) co-precipitation methods⁴.

simple hydrothermal process, the synthesis is typically carried out at moderate temperatures and high pressures, resulting in agglomerated nanocrystals. Many appropriate parameters such as working temperature, reaction conditions, solvents, surfactants, precursors and even structure-directing agents have been successfully employed to improve the properties of MON with high level of control of the shape, size distribution and crystallinity. Hydrothermal synthesis has been employed in obtaining metal oxides especially 1-D MON such as Al_2O_3 nanowires and VO_2 nanorods as well as porous metal oxide such as NiO.

2.3 Co-precipitation Method

Various nanoparticulate metal oxides can be synthesised by precipitation of the sparingly soluble products, formed under the condition of supersaturation, from aqueous solutions followed by thermal decomposition. The supersaturation condition requires that nucleation be a critical step in the synthesis method as a large number of particles will form simultaneously, which can subsequently undergo secondary processes such as Ostwald ripening and aggregation. In more complicated, the process becomes more complex, as multiple species must be precipitated simultaneously, hence the term co-precipitation. Just mere precipitation does not guarantee the formation of nanoparticulate structures. Co-precipitation is also known as wet chemical solution method. Several nanotextured of metal oxides have been synthesised using the co-precipitation method such as NiO nanoparticles, MgO nanoparticles, nanoflakes/nanofibers, and ellipsoidal shaped CuO nanoparticles.

3. PROPERTIES AND VARIOUS MON-BASED APPLICATIONS

MON systems have generated a considerable attention in recent past years for their potential to facilitate both fundamental research and practical applications through their advantageous chemical and physical properties. Development of MON is receiving considerable attention because of a rich spectrum of significant properties and advanced applications

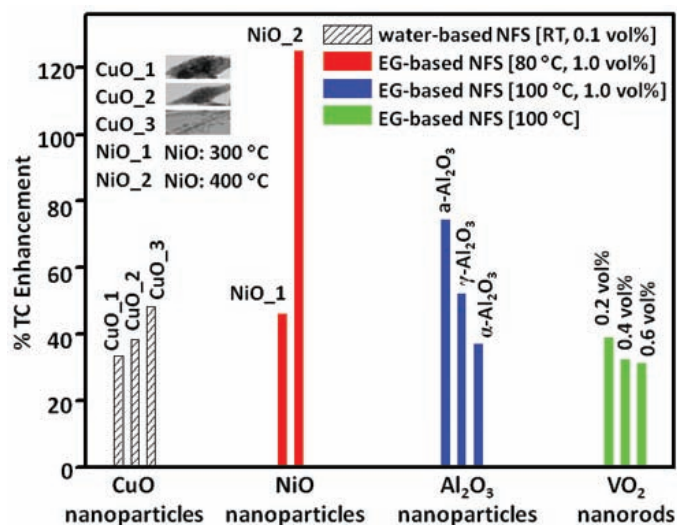


Figure 11. Histograms depicting a comparative study of some of thermal conductivity (TC) enhancement recorded for different MON based water and ethylene glycol (EG) nanofluids (NFs)^{11,21,50-51}.

in nanoscience and nanotechnology. Most of applications exploit their surface properties which are induced by different structural arrangements. The crystalline phases with the same size and shape can intrinsically alter the surface atomic configurations of the MON. The surface vacancies and lattice oxygen species may be simultaneously involved in the sensing performance, and the crystalline structure may change at the reaction temperature. Moreover, when electrons and holes in a semiconductor are confined to ultrasmall regions of space (normally 1 nm - 25 nm), the sensing, optical and electronic properties of the semiconductors become strongly size dependent.⁸²⁻⁸⁶ In this section, few fascinating properties and plausible advanced applications of MON are describe. The summary of various MON with their structural information is represented in Table 3.

Moreover, the applications of MON are presently under investigation on the field in a wide range of applications which are as follows:

Table 3. Summary of metal oxide nanostructures with their structural information

Metal oxide	Crystal structure	Space group; lattice parameters
CdO	Cubic (NaCl type, fcc)	$Fm\bar{3}m$; $a = b = c = 0.469$ nm
CuO	Monoclinic	$C2/c$; $a = 0.468$ nm, $b = 0.342$ nm, $c = 0.513$ nm, $\beta = 99.549^\circ$
NiO	Cubic (rocksalt)	$Fm\bar{3}m$; $a = b = c = 0.417$ nm
MgO	Cubic (rocksalt; NaCl, B1))	$Fm\bar{3}m$ $a = b = c = 0.419$ nm
ZnO	Hexagonal (wurtzite)	$P63/mc$; $a = 0.325$ nm, $c = 0.520$ nm
TiO ₂	Tetragonal (anatase phase), orthorhombic (brookite phase) hexagonal (rutile phase)	$141/amd$; $a = b = 0.377$ nm, $c = 0.948$ nm $Pbca$; $a = 0.919$ nm, $b = 0.546$ nm, $c = 0.515$ nm $P42/mnm$; $a = b = 0.458$ nm, $c = 0.295$ nm
SnO ₂	Tetragonal (rutile phase)	$P42/mnm$; $a = b = 0.474$ nm, $c = 0.318$ nm
Al ₂ O ₃	Cubic (γ -phase), orthorhombic (ι -phase), monoclinic (θ -phase), rhombohedral (α -phase)	$Fd\bar{3}m$ $a = b = c = 0.792$ nm $PBAM$; $a = 0.773$ nm, $b = 0.761$ nm, $c = 0.292$ nm $C2/m$; $a = 1.174$ nm, $b = 0.572$ nm, $c = 1.12$ nm, $\beta = 103.34^\circ$ $R\bar{3}c$ $a = b = 0.475$ nm, $c = 1.299$ nm
VO ₂	Monoclinic (VO ₂ (B) phase)	$C2/m$; $a = 1.206$ nm, $b = 0.369$ nm, $c = 0.642$ nm, $\beta = 106.98^\circ$

3.1 Humidity Sensors

Both the measurement and control of surrounding humidity are of great importance for various industrial and agricultural process control, human activities, meteorology, pharmaceuticals and food production. Owing to the high specific surface area, MON systems have been attracted substantial attention toward the development of humidity sensitive materials and wide range applications from observing food quality to meteorological and pharmaceutical studies. MON usually have both acidic and basic sites on oxide surfaces and stronger absorption ability than bulk materials due to larger surface-to-volume ratio, higher surface activity and better adsorption performance. This amphoteric nature of MON enhances the catalytic behaviour, which is highly useful in sensing and environmental monitoring. Due to water molecule chemisorption, however, ceramic-based humidity sensors still suffer from insufficient sensitivity over wide humidity ranges. Recently nanoparticulates metal oxides, e.g. SnO₂ nanoparticles and VO₂ nanorods, are continuing to be at the forefront of nano-science and technology due to large surface area and hollow interior space. Moreover, hollow nanotubes with controllable internal voids have revealed to superior sensing properties, because they not only increase efficient adsorption sites for water vapours, but also promote dissociation of water absorbed onto the surface of nanotube walls with high surface charge densities, so that sensitivity of sensor can be enhanced at low humidity. Porous MON also improve their practical application in the field of humidity sensing due to abundant void fraction. The presence of an adsorbed layer of water at the surface reduces the total sensor impedance due to the increase in ionic conductivity as well as capacitance due to high dielectric constant of water. The ability of both amorphous and crystalline MON to sense humidity is due to the large surface area available for water adsorption and high surface activity. Moreover, nanotubes and nanorods of MON also provide effective and fast channels for vapour and liquid transport. Therefore, sensors based on MON show high sensitivity and fast response time to humidity, are suitable for applications in environmental monitoring.

3.2 Gas Sensors

Another significant contemporary challenge in the area of gas-sensing performance is to develop efficient sensitivity MON with desirable properties correlated to controllable morphology. Gas sensors are commonly used for detecting gases like carbon monoxide (CO), methane (CH₄), and organic vapours like ethanol (C₂H₅OH). Since many gases (*e.g.* LPG, O₂, H₂, NO₂, NH₃, CH₄, CO, and ethanol) are harmful to human being and cause serious atmospheric pollution, therefore methods of gas sensing are developed as a part of a safety system. It is important to detect and monitor such gases. The nanostructures for gas sensing are mainly metal oxides because oxygen sites on their surfaces provide the possibility of gas adsorption. Smaller size of MON, higher gas sensitivity will be. 1-D semiconductors MON play a dominant role is solid state gas sensors and used as effective materials for gas and ethanol detection. Moreover, gas and ethanol sensors based on MON have also potential application in screening intoxicated

drivers, monitoring food and biomedical safety. The basic materials for thick film gas sensors are in general SnO₂ and ZnO, etc. The sensing properties of MON based sensors (sensitivity, selectivity and reproducibility) depend on several factors, mainly crystallite size and specific surface area. A gas sensor is a device which provides a platform to detect gases in different conditions. Gas sensors are used to detect combustible, flammable and toxic gases as well as to monitor oxygen depletion. Measurements usually involve the changes in conductivity and resistivity of material due to the presence of gas. Mechanism involves the adsorption of active gases on surface of MON that cause change in electrical conductivity. Consequently the use of MON increases gas sensitivity as well as decreases response time. The enhancement in sensor performance is probably nanosised grains of MON are almost depleted of carriers, most carriers are trapped in surface states, and they exhibit greater conductance changes as more carriers are activated from their trapped states to the conduction band than with microsised grains.

3.3 Defence Applications

Another intriguing aspect of MON could be potentially used in defence applications to protect the high valued defence data. Recent reports demonstrate that MON luminescent ink could be easily applied inexpensive way to different surfaces and have been implemented widely as security inks to print the security codes and bars for defence applications. Moreover, the applications of MON are presently under investigation in various fields include nanoparticulate of metal oxides to make smart coating, advanced computing power for code breaking and encryption, sensors to detect life, safety and emergency signs, nanosensors in light-weight uniforms, in the night or dark environment vision displays, as luminescent pigments used as luminous painting in watches and other instruments' dials⁸⁷⁻⁹⁰.

3.4 Optical Displays

Light is a form of energy and the harvesting of light requires any other form of energy which must be supplied to generate it. In luminescence some energy source promotes an electron within a material from a lower energy ground state to a higher energy excited state and the electron release to a lower energy state by releasing the energy in the form of light. The optical applications of MON are unparalleled and are recognised in various fields. Among these the photoluminescence (PL) is, initiated by photoexcitation (excitation by photons) luminescence, widely known for interpreting defects in both semiconductors and insulators. An optical transition occurs when a photon is absorbed or emitted by the defect. The visible emission is associated to defects-related emission, e.g. oxygen vacancies and metal interstitials. PL is a non-destructive, high-sensitivity and direct optical tool to study the surface oxygen vacancies, lattice defects, self-trapped and localised excitons and electronic energy band structure analysis in MON. Temperature is also an important parameter in carrier dynamics. Generally, at room temperature the probability of MON to exhibit luminescence depends on intrinsic band structure and other internal/external factors. When the temperature is sufficiently low, carriers will trapped

at surface or crystal defects, since crystalline imperfections are very efficient trapping centers and dominated by lowest energy levels, which appear in low-temperature PL spectrum. The intensity of PL spectra gradually increases with decreasing the temperature due to weakened nonradiative recombination. The luminescence spectra and corresponding luminescence decay times are directly related to the properties of MON. The decay time of luminescence of a material is an essential parameter for deciding its performance and applications in fast optical sensors. The efficiency of radiative recombination is directly proportional to decay time of particular transition. Optical displays/switches/sensors-based on MON require decay time to be in milliseconds to picoseconds range and are widely used in optoelectronics switching and bioimaging devices as well as LED application. Various nano-scaled morphologies and different phases of metal oxides, such as MgO nanoflakes/nanofibers, and Al₂O₃ nanoparticles and nanowires exhibit a fast decay time of luminescence of less than 10 ns, which suggests its proposed use in white light generation (a combination of blue and red emissions), solid-state lighting applications, optical sensors and various optoelectronic devices.

3.5 Thermal Conductivity of MON's Nanofluids

One of the great challenges in the present scenario in this field is unquestionably in proper energy management which could be improved in heat energy transfer so as to accommodate high-performance for efficient thermal flow management in industries such as microelectronics, transportation, chemical engineering, aerospace and manufacturing. Among the various shapes of nano-metal oxides, CuO nanostructures, e.g. seeds, ellipsoidal, rods and leaves, NiO nanoparticles, Al₂O₃ nanoparticles (both amorphous and crystalline (γ - and α -Al₂O₃) structures) and VO₂ nanorods showed their ability to enhance the thermal conductivity of water to a noticeable degree at high temperatures, even at very small concentrations.

4. FUTURE SCOPE OF MON

Among all the above discussed various morphology based MON (nano-particles, wires, rings, combs, tetrapods) such as CdO, CuO, NiO, MgO, ZnO, TiO₂, SnO₂, Al₂O₃, and VO₂ could be considered for need of an hour and production of it can fulfill the huge demand for its futuristic applications in sensing, optical and optoelectronic nano-devices. Hence, these nanostructures form the basis of nanotechnology applications in sensors and electronics for next generation high performance nanodevices. Since the inceptive studies of emerging nanomaterials in the early 2000s, a variety of nanomaterials with fascinating morphologies have been piqued the interests of material scientists because the higher surface-to-volume ratio and are beneficial to enhancement in the efficiency of surface reactions. Future research for the development of nanosystems is anticipated to take multiple directions such as new synthesis principles, new types of nanostructures and their trends for technological applications are expected to emerge. The application of MON in the design of highly sensitive sensing, optical sensors and optoelectronics devices with modifications of structures and properties, should receive increasing attention.

Keeping in view of the above discussions in present review it is clear that the various nano-scaled morphologies, different phases and the its suitable applications in various fields further stimulates scientific community to explore more MON for their potential use in advanced applications.

5. CONCLUSION

Authors proposed that the excellent sensing performance, good optical properties and low cost, such artificially engineered MON could be used as building blocks materials in next generation construction of nano-devices. Additionally, the present review covers the fundamental concepts of various types of MON and methodology to synthesise it to suitable applications. Once their unique properties have been understood and dominated, MON will offer vast and unforeseen opportunities in the fields of science and technology. We believe that the present review on the study of MON further reignites researchers to explore on MON for their enhanced use in advanced applications which will lead to rapid development of MON-based devices with excellent performance.

REFERENCES

1. Cheng, J.J.; Nicaise, S.M.; Berggren, K.K. & Gradečak, S. Dimensional tailoring of hydrothermally grown zinc oxide nanowire arrays. *Nano Lett.*, 2016, **16**, 753. doi: 10.1021/acs.nanolett.5b04625
2. Holmes, M.; Song, Z.; Moghimi, H.R. & Roberts, M.S. Relative penetration of zinc oxide and zinc ions into human skin after application of different zinc oxide formulations. *ACS Nano*, 2016, **10**, 1810. doi: 10.1021/acsnano.5b04148
3. Baum, Peter; Yang, Ding-Shyue & Zewail, Ahmed H. 4D visualization of transitional structures in phase transformations by electron diffraction. *Science*, 2007, **318**, 788. doi: 10.1126/science.1147724
4. Gangwar, J.; Gupta, B.K.; Tripathi S.K. & Srivastava, A.K. Phase dependent thermal and spectroscopic responses of Al₂O₃ nanostructures with different morphogenesis. *Nanoscale*, 2015, **7**, 13313. doi: 10.1039/C5NR02369F
5. Fröschl, T.; Hörmann, U.; Kubiak, P.; Kučerová, G.; Pfanzelt, M.; Weiss, C.K.; Behm, R.J.; Hüsing, N.; Kaiser, U.; Landfester, K. & Wohlfahrt-Mehrens, M. High surface area crystalline titanium dioxide: potential and limits in electrochemical energy storage and catalysis. *Chem. Soc. Rev.*, 2012, **41**, 5313. doi: 10.1039/c2cs35013k
6. McWilliams, R.S.; Spaulding, D.K.; Eggert, J.H.; Celliers, P.M.; Hicks, D.G.; Smith, R.F.; Collins, G.W. & Jeanloz, R. Phase transformations and metallization of magnesium oxide at high pressure and temperature. *Science*, 2012, **338**, 1330. doi: 10.1126/science.1229450
7. Li, Y. & Shen, W. Morphology-dependent nanocatalysts: Rod-shaped oxides. *Chem. Soc. Rev.*, 2014, **43**, 1543. doi: 10.1039/C3CS60296F
8. McFarland, E.W. & Metiu, H. Catalysis by doped oxides. *Chem. Rev.*, 2013, **113**, 4391. doi: 10.1021/cr300418s
9. Czerwińska, M. Military nanomaterials applications. *Chemik*, 2014, **68**, 536.

10. Liu, K.; Cao, M.; Fujishima, A. & Jiang, L. Bio-inspired titanium dioxide materials with special wettability and their applications. *Chem. Rev.*, 2014, **114**, 10044. doi: 10.1021/cr4006796
11. Gangwar, J.; Dey, K.K.; Tripathi, S.K.; Wan, M.; Yadav, R.R.; Singh, R.K.; Samta & Srivastava, A.K. NiO-based nanostructures with efficient optical and electrochemical properties for high-performance nanofluids. *Nanotechnology*, 2013, **24**, 415705. doi: 10.1088/0957-4484/24/41/415705
12. Patra, A.K.; Dutta, A. & Bhaumik, A. Self-assembled mesoporous γ -Al₂O₃ spherical nanoparticles and their efficiency for the removal of arsenic from water. *J. Hazard. Mater.*, 2012, **201-202**, 170. doi: 10.1016/j.jhazmat.2011.11.056
13. Zeng, J.; Li, R.; Liu, S. & Zhang, L. Fiber-like TiO₂ nanomaterials with different crystallinity phases fabricated via a green pathway. *ACS Appl. Mater. Interfaces*, 2011, **3**, 2074. doi: 10.1021/am200297b
14. Reddy, M.V.; Subba Rao, G.V. & Chowdari, B.V.R. Metal oxides and oxysalts as anode materials for Li ion batteries. *Chem. Rev.*, 2013, **113**, 5364. doi: 10.1021/cr3001884
15. Nie, Z.; Petukhova, A. & Kumacheva, E. Properties and emerging applications of self-assembled structures made from inorganic nanoparticles. *Nat. Nanotechnol.*, 2010, **5**, 15. doi: 10.1038/nnano.2009.453
16. Wang, X.; Yu, L.; Hu, P. & Yuan F. Synthesis of single-crystalline hollow octahedral NiO. *Cryst. Growth Des.*, 2007, **7**, 2415. doi: 10.1021/cg060957z.
17. Chen, Z.; Pan, D.; Li, Z.; Jiao, Z.; Wu, M.; Shek, C.H.; Wu, C.M.L. & Lai, J.K.L. Recent advances in tin dioxide materials: some developments in thin films, nanowires, and nanorods. *Chem. Rev.*, 2014, **114**, 7442. doi: 10.1021/cr4007335
18. Gangwar, J.; Dey, K.K.; Komal, P.; Tripathi S.K. & Srivastava, A.K. Microstructure, phase formations and optical bands in nanostructured alumina. *Adv. Mater. Lett.*, 2011, **2**, 402. doi: 10.5185/amlett.2011.3233
19. Pan, Z.W.; Dai, Z.R. & Wang, Z.L. Nanobelts of semiconducting oxides. *Science*, 2001, **291**, 1947. doi: 10.1126/science.1058120
20. Valencia, P. M.; Farokhzad, O.C.; Karnik, R. & Langer, R. Microfluidic technologies for accelerating the clinical translation of nanoparticles. *Nat. Nanotechnol.*, 2012, **7**, 623. doi: 10.1038/nnano.2012.168
21. Gangwar, J.; Srivastava, A.K.; Tripathi, S.K.; Wan, M. & Yadav, R.R. Strong enhancement in thermal conductivity of ethylene glycol-based nanofluids by amorphous and crystalline Al₂O₃ nanoparticles. *Appl. Phys. Lett.*, 2014, **105**, 063108. doi: 10.1063/1.4893026
22. Shang, S.; Xue, K.; Chen, D. & Jiao, X. Preparation and characterization of rose-like NiO nanostructures. *Cryst. Eng. Comm.*, 2011, **13**, 5094. doi: 10.1039/c0ce00975j
23. Zhong, L.S.; Hu, J.S.; Liang, H.P. ; Cao, A.M.; Song, W.G. & Wan, L.J. Self-assembled 3D flowerlike iron oxide nanostructures and their application in water treatment. *Adv. Mater.*, 2006, **18**, 2426. doi: 10.1002/adma.200600504
24. Srivastava, A.K.; Praveen; Arora, M.; Gupta, S.B.K.; Chakraborty, B.R.; Chandra, S.; Toyoda, S. & Bahadur, H. Nanostructural features and optical performance of RF magnetron sputtered ZnO thin films. *J. Mater. Sci. Technol.*, 2010, **26**, 986. doi: 10.1016/S1005-0302(10)60161-2
25. Cheng, Tian, B.; Xie, C.; Xiao, Y. & Lei, S. Highly sensitive humidity sensor based on amorphous Al₂O₃ nanotubes. *J. Mater. Chem.*, 2011, **21**, 1907. doi: 10.1039/C0JM02753G
26. Zhang, H.; Guo, L. & Wan, Q. Nanogranular Al₂O₃ proton conducting films for low-voltage oxide-based homojunction thin-film transistors. *J. Mater. Chem. C*, 2013, **1**, 2781. doi: 10.1039/c3tc30137k
27. Wu, X.; Xiong, S.; Guo, J.; Wang, L.; Hua, C.; Hou, Y. & Chu, P. K. Ultrathin amorphous alumina nanoparticles with quantum-confined oxygen-vacancy-induced blue photoluminescence as fluorescent biological labels. *J. Phys. Chem. C*, 2012, **116**, 2356. doi: 10.1021/jp210599z
28. Gangwar, J.; Gupta, B.K. ; Kumar, P.; Tripathi, S.K. & Srivastava, A.K. Time-resolved and photoluminescence spectroscopy of θ -Al₂O₃ nanowires for promising fast optical sensor applications. *Dalton Trans.*, 2014, **43**, 17034. doi: 10.1039/C4DT01831A
29. Joshi, T.; Prakash, J.; Kumar, A.; Gangwar, J.; Srivastava, A.K.; Singh, S. & Biradar, A. M. Alumina nanoparticles find an application to reduce the ionic effects of ferroelectric liquid crystal. *J. Phys. D: Appl. Phys.*, 2011, **44**, 315404. doi: 10.1088/0022-3727/44/31/315404
30. Hong, H.; Wang, F.; Zhang, Y.; Graves, S. A.; Eddine, S. B.Z.; Yang, Y.; Theuer, C.P.; Nickles, R.J.; Wang, X. & Cai, W. Red fluorescent zinc oxide nanoparticle: a novel platform for cancer targeting. *ACS Appl. Mater. Interfaces*, 2015, **7**, 3373. doi: 10.1021/am508440j
31. Adak, Bandyopadhyay, M. & Pal, A. Removal of crystal violet dye from wastewater by surfactant-modified alumina. *Sep. Purif. Technol.*, 2005, **44**, 139. doi: 10.1016/j.seppur.2005.01.002
32. Fang, X.S.; Ye, C.H.; Peng, X. S.; Wang, Y.H.; Wu, Y.C. & Zhang, L.D. Temperature-controlled growth of α -Al₂O₃ nanobelts and nanosheets. *J. Mater. Chem.*, 2003, **13**, 3040. doi: 10.1039/B309193G
33. Srivastava, A.K.; Deepa, M.; Sood, K.N.; Erdem, E. & Eichel, R.A. Shape selective growth of ZnO nanostructures: spectral and electrochemical response. *Adv. Mat. Lett.*, 2011, **2**, 142. doi: 10.5185/amlett.2011.1201
34. Kumar, G.; Kedawat, P.; Kumar, J.; Dwivedi & Gupta, B. K. Sunlight-activated Eu²⁺/Dy³⁺ doped SrAl₂O₄ water resistant phosphorescent layer for optical displays and defence applications. *New J. Chem.*, 2015, **39**, 3380. doi: 10.1039/C4NJ02333A
35. Jain, P.; Singh, S. & Siddiqui, A. M. Tin oxide thin films prepared by thermal evaporation technique under different vacuum conditions. *Adv. Sci. Eng. Med.*, 2012, **4**, 230. doi: 10.1166/asem.2012.1177.
36. Chou, J.Y.; Falk, J.L.L.; Hemesath, E.R. & Lathon, L.J. J. Vanadium oxide nanowire phase and orientation analyzed by Raman spectroscopy. *Appl. Phys.*, 2009, **105**, 034310. doi: 10.1063/1.3075763

37. Gangwar, J.; Srivastava, A.K. & Tripathi, S.K. Size controlled synthesis and evaluation of optical properties of alumina nanoparticles. *AIP Conf. Proc.*, 2011, **1393**, 379. doi: 10.1063/1.3653768
38. Zhu, Q.; Oganov, A.R. & Lyakhov, A.O. Novel stable compounds in the Mg-O system under high pressure. *Phys. Chem. Chem. Phys.*, 2013, **15**, 7696. doi: 10.1039/c3cp50678a
39. Gangwar, J.; Chandran, A.; Joshi, T.; Verma, R.; Biradar, A.M.; Tripathi, S.K.; Gupta, B.K. & Srivastava, A.K. Probing on phase dependent luminescent properties of Al₂O₃ nanowires for their performance in ferroelectric liquid crystal. *Mater. Res. Express*, 2015, **2**, 075013. doi: 10.1088/2053-1591/2/7/075013
40. Devan, R.S.; Patil, R.A.; Lin, J.H. & Ma, Y.R. One-dimensional metal-oxide nanostructures: recent developments in synthesis, characterization, and applications. *Adv. Funct. Mater.*, 2012, **22**, 3326. doi: 10.1002/adfm.201201008
41. Shao, J.; Li, X.; Qu, Q.; Zheng, H. One-step hydrothermal synthesis of hexangular starfruit-like vanadium oxide for high power aqueous supercapacitors. *J. Power Sources*, 2012, **219**, 253. doi: 10.1016/j.jpowsour.2012.07.045
42. Huang, J. & Wan, Q. Gas sensors based on semiconducting metal oxide one-dimensional nanostructures. *Sensors*, 2009, **9**, 9903. doi: 10.3390/s91209903
43. Kumar, P.; Dwivedi, J. & Gupta, B.K. Highly luminescent dual moderate-rare-earth nanorod assisted multi-stage excitable security ink for anticounterfeiting applications. *J. Mater. Chem. C*, 2014, **2**, 10468. doi: 10.1039/C4TC02065K
44. Bahadur, H.; Samanta, S.B.; Srivastava, A.K.; Sood, K.N.; Kishore, R.; Sharma, R.K.; Basu, A.; Rashmi, Kar, M.; Pal, P.; Bhatt, V. & Chandra, S. Nano and micro structural studies of thin films of ZnO. *J. Mater. Sci.*, 2006, **41**, 7562. doi: 10.1007/s10853-006-0841-x
45. Srivastava, A.K.; Chakraborty, B.R. & Chandra, S. Crystallographically oriented nanorods and nanowires of RF-magnetron-sputtered zinc oxide. *J. Nanomater.*, 2009, **2009**, 310360. doi: 10.1155/2009/310360.
46. Datt, R.; Gangwar, J.; Tripathi, S. K.; Singh, R. K. & Srivastava, A.K. Porous nickel oxide nanostructures for supercapacitor applications. *Quantum Matter*, 2016, **5**, 1.
47. Jamwal, G.; Prakash, J.; Chandran, A.; Gangwar, J.; Srivastava, A.K. & Biradar, A. M. Effect of nickel oxide nanoparticles on dielectric and optical properties of nematic liquid crystal. *AIP Conf. Proc.*, 2015, 1675, 030065. doi: 10.1063/1.4929281.
48. Srivastava, A.K.; Gupta, N.; Lal, K.; Sood, K.N. & Kishore, R. Effect of variable pressure on growth and photoluminescence of ZnO nanostructures. *J. Nanosci. Nanotechnol.*, 2007, **7**, 1. doi:10.1166/jnn.2007.745.
49. JLin, C.; Yu, M.; Cheng, Z.; Zhang, C.; Meng, Q. & Lin J. Bluish-white emission from radical carbonyl impurities in amorphous Al₂O₃ prepared via the pechini-type sol-gel process. *Inorg. Chem.*, 2008, **47**, 49. doi: 10.1021/ic700652v
50. Dey, K.K.; Kumar, A.; Shanker, R.; Dhawan, A.; Wan, M.; Yadav, R.R. & Srivastava, A.K. Growth morphologies, phase formation, optical & biological responses of nanostructures of CuO and their application as cooling fluid in high energy density devices. *RSC Adv.*, 2012, **2**, 1387. doi: 10.1039/c1ra00710f..
51. Dey, K.K.; Bhatnagar, D.; Srivastava, A.K.; Wan, M.; S. Singh, Yadav, R. R.; Yadav, B. C. & Deepa, M. VO₂ nanorods for efficient performance in thermal fluids and sensors. *Nanoscale*, 2015, **7**, 6159. doi: 10.1039/C4NR06032F
52. Li, J.; Su, Z.; Yang, B.; Cai, S.; Dong, Z.; Man, J. & Li, R. A facile and environmentally friendly chemical route for the synthesis of metastable VO₂ nanobelts. *J. Phys. Chem. Solids*, 2010, **71**, 407. doi: 10.1016/j.jpcs.2009.12.075
53. Srivastava, A.; Jain, K.; Rashmi, A.; Srivastava, A.K. & Lakshmikumar, S.T. Study of structural and microstructural properties of SnO₂ powder for LPG and CNG gas sensors. *Mater. Chem. Phys.*, 2006, **97**, 85. doi: 10.1016/j.matchemphys.2005.07.065
54. Singh, P.; Sinha, O.P.; Srivastava, R.; Srivastava, A.K.; Bindra, J.K.; Singh, R.P. & Kamalasanan, M.N. Studies on morphological and optoelectronic properties of MEH-CN-PPV:TiO₂ nanocomposites. *Mater. Chem. Phys.*, 2012, **133**, 317. doi: 10.1016/j.matchemphys.2012.01.030
55. Srivastava, A.K.; Deepa, M.; Bahadur, N. & Goyat, M. S. Influence of Fe doping on nanostructures and photoluminescence of sol-gel derived ZnO. *Mater. Chem. Phys.*, 2009, **114**, 194. doi: 10.1016/j.matchemphys.2008.09.005
56. Song, X.; Gao, L. & Mathur S. Synthesis, characterization, and gas sensing properties of porous nickel oxide nanotubes. *J. Phys. Chem. C*, 2011, **115**, 21730. doi: 10.1021/jp208093s
57. Srivastava, A.K.; Pandey, S.; Sood, K.N.; Halder, S.K. & Kishore, R. Novel growth morphologies of nano- and micro-structured cadmium oxide. *Mater. Lett.*, 2008, **62**, 727. doi: 10.1016/j.matlet.2007.06.044
58. Srivastava, A.K. Direct evidence for electron beam irradiation-induced phenomena in nanowired ZnO thin films. *Mater. Lett.*, 2008, **62**, 4296. doi: 10.1016/j.matlet.2008.07.009
59. Jain, N.; Marwaha, N.; Verma, R.; Gupta, B.K. & Srivastava, A.K. Facile synthesis of defect-induced highly luminescent pristine MgO nanostructures for promising solid-state lighting applications. *RSC Adv.*, 2016, **6**, 4960. doi: 10.1039/c5ra21150f.
60. Verma, R.; Naik, K.K.; Gangwar, J. & Srivastava, A.K. Morphology, mechanism and optical properties of nanometer-sized MgO synthesized via facile wet chemical method. *Mater. Chem. Phys.*, 2014, **148**, 1064. doi: 10.1016/j.matchemphys.2014.09.018
61. Srivastava, A.K.; Deepa, M.; Bhandari, S. & Fuess, H. Tunable nanostructures and crystal structures in titanium oxide films. *Nanoscale Res. Lett.*, 2009, **4**, 54. doi: 10.1007/s11671-008-9202-9
62. Bahadur, H.; Srivastava, A.K.; Sharma, R.K. & Chandra, S. Morphologies of sol-gel derived thin films of ZnO using different precursor materials and their nanostructures. *Nanoscale Res. Lett.*, 2007, **2**, 469. doi: 10.1007/s11671-

- 007-9089-x
63. Srivastava, A.K.; Ninagawa, K.; Toyoda, S.; Chakraborty, B.R. & Chandra, S. Induced thermoluminescence of X-ray irradiated nanostructured zinc oxide. *Opt. Mater.*, 2009, **32**, 410. doi: 10.1016/j.optmat.2009.09.007
 64. Tawale, J.S.; Kumar, A.; Mohan, A. & Srivastava, A.K. Influence of silver and graphite on zinc oxide nanostructures for optical application. *Opt. Mater.*, 2013, **35**, 1335. doi: 10.1016/j.optmat.2013.01.034
 65. Abeykoon, M.M.; Colin, M.C.; Anokhina, E.V.; Iliiev, M.N.; Donner, W.; Jacobson, A.J. & Moss, S.C. Synchrotron x-ray and optical studies of the structure of HgSe semiconductor nanoclusters confined in zeolite L and zeolite Y. *Phys. Rev. B*, 2008, **77**, 075333. doi: 10.1103/PhysRevB.77.075333
 66. Pacchioni, G. Two-dimensional oxides: multifunctional materials for advanced technologies. *Chem. Eur. J.*, 2012, **18**, 10144. doi: 10.1002/chem.201201117
 67. Gangwar, J.; Kim, J.; Kumar, A.; Bhatnagar, D.; Senthil, K.; Tripathi, S.K.; Yung, K. & Srivastava, A.K. Optimization control on growth morphology, lattice scale features and optical response of Al-incorporated ZnO nano-needles. *Nanosci. Nanotechnol. Lett.*, 2013, **5**, 67. doi: 10.1166/nl.2013.1429
 68. Verma, R.; Mantri, B.; Ramphal & Srivastava, A.K. Shape control synthesis, characterizations, mechanisms and optical properties of large scaled metal oxide nanostructures of ZnO and TiO₂. *Adv. Mater. Lett.*, 2015, **6**, 324. doi: 10.5185/amlett.2015.5661.
 69. Rinke, P.; A. Schleife, Kioupakis, E. ; Janotti, A.; Rödl, C.; Bechstedt, F.; Scheffler, M. & C. Walle, G. V. First-principles optical spectra for F centers in MgO. *Phys. Rev. Lett.*, 2012, **108**, 126404. doi: 10.1103/PhysRevLett.108.126404
 70. Haertelt, M.; Fielicke, A.; Meijer, G.; Kwapien, K.; Sierkaz, M. & Sauer, J. Structure determination of neutral MgO clusters-hexagonal nanotubes and cages. *Phys. Chem. Chem. Phys.*, 2012, **14**, 2849. doi: 10.1039/c2cp23432g
 71. Zhang, Y.G.; He, H.Y. & Pan, B.C. Structural features and electronic properties of MgO nanosheets and nanobelts. *J. Phys. Chem. C*, 2012, **116**, 23130. doi: 10.1021/jp3077062
 72. Zhang, X.; Shi, W.; Zhu, J.; Zhao, W.; Ma, J.; Mhaisalkar, S.; Maria, T. L.; Yang, Y.; Zhang, H.; Hng, H. H. & Yan Q. Synthesis of porous NiO nanocrystals with controllable surface area and their application as supercapacitor electrodes. *Nano Res.*, 2010, **3**, 643. doi: 10.1007/s12274-010-0024-6
 73. Lodziana, Z.; Topsøe, N.Y. & Nørskov, J.K. A negative surface energy for alumina. *Nat. Mater.*, 2004, **3**, 289. doi: 10.1038/nmat1106
 74. Yan, L.; Zhuang, J.; Sun, X.; Den, Z. & Li, Y. Formation of rod-like Mg(OH)₂ nanocrystallites under hydrothermal conditions and the conversion to MgO nanorods by thermal dehydration. *Mater. Chem. Phys.*, 2002, **76**, 119. doi: 10.1016/S0254-0584(01)00509-0
 75. Zhu, W.; Zhang, L.; Tian, G.L.; Wang, R.; Zhang, H.; Piao, X. & Zhang, Q. Flux and surfactant directed facile thermal conversion synthesis of hierarchical porous MgO for efficient adsorption and catalytic growth of carbon nanotubes. *Cryst. Eng. Comm.*, 2014, **16**, 308. doi: 10.1039/C3CE41394B
 76. Luan, F.; Wang, G.; Ling, Y.; Lu, X.; Wang, H.; Tong, Y.; Liu, X. X. & Li Y. High energy density asymmetric supercapacitors with a nickel oxide nanoflake cathode and a 3D reduced graphene oxide anode. *Nanoscale*, 2013, **5**, 7984. doi: 10.1039/c3nr02710d
 77. Dey, K.K.; Kumar, P.; Yadav, R.R.; Dhar, A. & Srivastava, A.K. CuO nanoellipsoids for superior physicochemical response of biodegradable PVA. *RSC Adv.*, 2014, **4**, 10123. doi: 10.1039/c3ra46898d.
 78. Tawale, J.S.; Gupta, G.; Mohan, A.; Kumar, A. & Srivastava, A.K. Growth of thermally evaporated SnO₂ nanostructures for optical and humidity sensing application. *Sensor. Actuat. B-Chem.*, 2014, **201**, 369. doi: 10.1016/j.snb.2014.04.099
 79. Aryal, S.; Rulis, P.; Ouyang, L. & Ching W. Y. Structure and properties of the low-density phase α -Al₂O₃ from first principles. *Phys. Rev. B*, 2011, **84**, 174123. doi: 10.1103/PhysRevB.84.174123
 80. Ganguly, A.; Anjaneyulu, O.; Ojha, K. & Ganguli, A.K. Oxide-based nanostructures for photocatalytic and electrocatalytic applications. *Cryst. Eng. Comm.*, 2015, **17**, 8978. doi: 10.1039/C5CE01343G
 81. Zhang, J.; Wu, Y.; Xing, M.; Leghari, S.A.K. & Sajjad, S. Development of modified N doped TiO₂ photocatalyst with metals, nonmetals and metal oxides. *Energy Environ. Sci.*, 2010, **3**, 715. doi: 10.1039/b927575d
 82. Khan, M.M.; Ansari, S.A.; Pradhan, D.; Ansari, M.O.; Han, D.H.; Lee, J. & Cho, M.H. Band gap engineered TiO₂ nanoparticles for visible light induced photoelectrochemical and photocatalytic studies. *J. Mater. Chem. A*, 2014, **2**, 637. doi: 10.1039/C3TA14052K
 83. Kumari, L.; Li, W. Z.; Vannoy, C. H.; Leblanc, R. M. & Wang D. Z. Vertically aligned and interconnected nickel oxide nanowalls fabricated by hydrothermal route. *Cryst. Res. Technol.*, 2009, **44**, 495. doi: 10.1002/crat.200800583
 84. Dai, Z. R.; Pan, Z. W. & Wang, Z. L. Novel nanostructures of functional oxides synthesized by thermal evaporation. *Adv. Funct. Mater.*, 2003, **13**, 9. doi: 10.1002/adfm.200390013
 85. Li, C.; Kawaharamura, T.; Matsuda, T.; Furuta, H.; Hiramatsu, T.; Furuta, M. & Hirao, T. Intense green cathodoluminescence from low temperature-deposited ZnO film with fluted hexagonal cone nanostructures. *Appl. Phys. Exp.*, 2009, **2**, 091601. doi: 10.1143/APEX.2.091601
 86. Dey, K.K. & Srivastava, A.K. Oxide Nanostructures: Growth, Microstructures, and Properties, edited by A. K. Srivastava. Pan Stanford Publishing, 2014, **1**, pp. 1-98.
 87. Gupta, B. K.; Harnath, D. ; Saini, S. ; Singh, V. N. & Shanker, V. Synthesis and characterization of ultra-fine Y₂O₃:Eu³⁺ nanophosphors for luminescent security ink applications. *Nanotechnology*, 2010, **21**, 055607. doi:

10.1088/0957-4484/21/5/055607

88. Gupta, B.K.; Kumar, A.; Kumar, P.; Dwivedi, J.; Pandey, G.N. & Kedawat, G. Probing on green long persistent $\text{Eu}^{2+}/\text{Dy}^{3+}$ doped $\text{Sr}_3\text{SiAl}_4\text{O}_{11}$ emerging phosphor for security applications. *J. Appl. Phys.*, 2015, **117**, 243104. doi: 10.1063/1.4922983
89. Gupta, B.K.; Grover, V.; Gupta, G. & Shanker, V. Highly efficient luminescence from hybrid structures of ZnO/multi-walled carbon nanotubes for high performance display applications. *Nanotechnology*, 2010, **21**, 475701. doi: 10.1088/0957-4484/21/47/475701
90. Gupta, B.K.; Harnath, D.; Chawla, S.; Chander, H.; Singh, V.N. & Shanker, V. Self-catalytic synthesis, structure and properties of ultra-fine luminescent ZnO nanostructures for field emission application. *Nanotechnology*, 2010, **21**, 225709. doi: 10.1088/0957-4484/21/22/225709

ACKNOWLEDGEMENTS

The authors sincerely thank the Director, Prof. D.K. Aswal, CSIR-NPL New Delhi, India for providing the necessary infrastructural facilities. Mr Jitendra Gangwar would like to thanks Prof. K.S. Sharma and Dr Nidhi Bhargava of The IIS University, Jaipur for their encouragement and support. The projects, NanoSHE (BSC-0112) and DST (SR/NM/NS-97/2010), are gratefully acknowledged.

CONTRIBUTORS

Dr Jitendra Gangwar has obtained his PhD in Physics from Panjab University, Chandigarh, India. Presently, he is Assistant Professor, Department of Physics, The IIS University, Jaipur. His research interest is based on the understanding of microstructures, phase transformations, nucleation and growth mechanisms of metal oxide nanomaterials with their intriguing structural, electrochemical and optical properties for supercapacitor, optoelectronic and fast optical switches or optical sensors applications.

Dr Bipin Kumar Gupta received his PhD in Physics, from Banaras Hindu University, Varanasi, Uttar Pradesh, India in 2004. Presently he is Scientist in CSIR-National Physical Laboratory, New Delhi, India. He is a recipient of INDO-US fellowship in Physical Sciences (2010-11). He has more than 85 publications in reputable international journals. His current research interests are luminescent materials (0-D, 1-D, 2-D and 3D) for applications in invisible luminescent security ink, security codes, optoelectronic devices, biological fluorescence labeling, fluorescence quenching, luminescent paint, field emission displays and luminomagnetic nanophosphors for drug delivery and magnetic tracking.

Dr A.K. Srivastava did PhD (Metallurgy) at IISc Bangalore, MTech (Materials Science) at IIT, Kanpur and MSc (Physics) at IIT, Roorkee. He works on advanced materials, in particular on nanomaterials. He has published more than 200 articles in journals and presented more than 200 papers in scientific meetings. He is the recipient of: *Metallurgist of the Year Award – 2011* by the Government of India, *Materials Research Society of India Medal-2011*, and *INSA-KOSEF Fellowship* of the Governments of India & South Korea in 2009.